Université de Montréal

Dodecyltrimethylammonium chloride adsorption at the silica/water interface studied by Sum Frequency Generation

par
Lady Lorena Torres Chivara

Département de chimie
Faculté des arts et des sciences

Mémoire présenté à la Faculté des études supérieures et postdoctorales
en vue de l'obtention du grade de maître ès sciences (M.Sc.)
en chimie

Décembre 2015

Résumé

La génération des fréquences somme (SFG), une technique spectroscopique spécifique aux interfaces, a été utilisée pour caractériser les changements de la structure macromoléculaire du surfactant cationique chlorure de dodécyltriméthylammonium (DTAC) à l'interface silice/eau dans une plage de pH variant entre 3 et 11. Les conditions expérimentales ont été choisies pour imiter les conditions les plus communes trouvées pendant les opérations de récupération assistée du pétrole**.** Particulièrement, la silice a été étudiée, car elle est un des composantes des surfaces minérales des réservoirs de grès, et l'adsorption du surfactant a été étudiée avec une force ionique pertinente pour les fluides de la fracturation hydraulique. Les spectres SFG ont présenté des pics détectables avec une amplitude croissante dans la région des étirements des groupes méthylène et méthyle lorsque le pH est diminué jusqu'à 3 ou augmenté jusqu'à 11, ce qui suggère des changements de la structure des agrégats de surfactant à l'interface silice/eau à une concentration de DTAC au-delà de la concentration micellaire critique. De plus, des changements dans l'intensité SFG ont été observés pour le spectre de l'eau quand la concentration de DTAC augmente de 0,2 à 50 mM dans les conditions acide, neutre et alcaline. À pH 3, près du point de charge zéro de la surface de silice, l'excès de charge positive en raison de l'adsorption du surfactant cationique crée un champ électrostatique qui oriente les molécules d'eau à l'interface. À pH 7 et 11, ce qui sont des valeurs au-dessus du point de charge zéro de la surface de silice, le champ électrostatique négatif à l'interface silice/eau diminue par un ordre de grandeur avec l'adsorption du surfactant comme résultat de la compensation de la charge négative à la surface par la charge positive du DTAC. Les

résultats SFG ont été corrélés avec des mesures de l'angle de contact et de la tension interfaciale à pH 3, 7 et 11.

Mots clés : Spectroscopie nonlinéaire, surfactants d'alkylammonium, interfaces minéraux/eau, mouillabilité, tension interfaciale, fracturation hydraulique.

Abstract

Sum Frequency Generation (SFG), an interface specific spectroscopic technique, was used to characterize the changes in the macromolecular structure of the cationic surfactant dodecyltrimethylammonium chloride (DTAC) at the silica/water interface at pH values ranging from 3 to 11. The experimental conditions were selected to mimic conditions common during enhanced oil recovery operations. In particular, silica was studied since it is one of the most abundant mineral components of sandstone reservoirs, and surfactant adsorption was studied at an ionic strength (100 mM NaCl) relevant to hydraulic fracturing fluids. SFG spectra showed detectable peaks with increasing amplitude in the methylene and methyl stretching region when the pH was lowered to 3 or increased to 11, suggesting changes in the surfactant aggregate structure at the silica/water interface at a DTAC concentration above the critical micelle concentration. In addition, changes in the SFG intensity were observed for the water spectrum when increasing the DTAC concentration from 0.2 to 50 mM under acidic, neutral or alkaline conditions. At pH 3, near the point of zero charge of the silica surface, the excess positive charge due to adsorption of the cationic surfactant creates an electrostatic field that orients water molecules at the interface. At pH 7 and 11, which are above the point of zero charge of the silica surface, the negative electrostatic field at the silica/water interface decreases in magnitude with surfactant adsorption due to compensation of the negative surface charge by the positively charged DTAC. The SFG results were correlated with contact angle and interfacial tension measurements at pH 3, 7 and 11.

Keywords: Nonlinear Spectroscopy, Alkylammonium Surfactants, Mineral/Water Interfaces, Wettability, Interfacial Tension, Hydraulic Fracturing.

Table of contents

List of tables

List of figures

List of abbreviations

$\langle\alpha^{(3)}\rangle$ - third order polarizability

$\langle\alpha^{2}\rangle$ - second order polarizability

° - contact angle unit

A_v – Intensity of the vibrational modes

CH_2 – methylene groups

CH_3 – methyl groups

CH_3/CH_2 – methyl to methylene amplitude ratio

cm^{-1} – wavenumber unit

CMC – critical micelle concentration

CO_2 – carbon dioxide

CTAB – Cetyltrimethylammonium bromide

CTAC – Cetyltrimethylammonium chloride

d^+- methylene symmetric stretch

d^+_{FR} – methylene symmetric stretch (Fermi resonance)

D_2O – deuterated water

DCl – Deuterated hydrochloric acid

DTAB – Dodecyltrimethylammonium bromide

DTAB-d_{25} - dodecyl-d_{25}-trimethylammonium bromide. The surfactant tail was deuterated.

DTAC - Dodecyltrimethylammonium chloride

E_{IR} –Electric field generated by the infrared frequency

E_o – Electrostatic field

EOR – Enhanced oil recovery

E_{VIS} –Electric field generated by the visible frequency

h – hour

HCl- hydrochloric acid

HPLC – High performance liquid chromatography

M- moles per liter

min – minute

mM - millimoles per liter

mTorr – millitorr

mV – millivolts

MW – molecular weight

N –number density of molecules

NaCl – Sodium chloride

NaOD – Sodium deuterated hydroxide

NaOH – Sodium hydroxide

nm- nanometer

OH^- - hydroxyl

pK_a – logarithm of the acidity constant

PMMA - poly(methyl methacrylate)

P_{SFG} – Sum frequency generation polarization

PZC – point of zero charge

r^+ - methyl symmetric stretch

r^+_{FR} – methyl symmetric stretch (Fermi resonance)

r^+_{HG} - methyl symmetric stretch of the headgroup

SFG - Sum frequency generation

SHG - Second harmonic generation

-SiO^- - ionized silanol group

-SiOH – Silanol groups

-$SiOH_2^+$- protoned silanol group

TOC - total organic carbon

Γ_v - is the line with of the transition

$\chi^{(2)}$- second order susceptibility

$\chi^{(2)}_{NR}$ – nonresonant susceptibility

$\chi^{(2)}_{R}$ -resonant susceptibility

$\chi^{(3)}$ – third order susceptibility

XPS - X-ray photoelectron spectroscopy

ω_{IR} – Infrared frequency

ω_{SFG} – Sum frequency generation frequency

ω_{VIS} – Visible frequency

ζ potential – zeta potential

To Elisa, Luis, Maye and Betito

Acknowledgements

I express my sincere acknowledgement to my advisor, Professor Patrick Hayes, for all the support and the patience he dedicated during my Master study. His ethics, guidance and experience helped me to overcome the difficulties and he became a mentor and a model to follow in my professional life.

Special thanks to Prof. Paula Wood-Adams for providing us the access to Concordia University´s SFG system. To Profs. Jean-François Masson and Kevin Wilkinson for allowing me to use some of their equipment during my project. I must also thank the University of Montreal and especially the Faculté des Études Supérieures et Postdoctorales for the scholarship to conclude my studies.

Many thanks to the interns and students that I once worked with in my group, for their kind and generous help: Mathilde, Toufik, Amara, Mounia, Adriana, Philippe and Prettiny. I must also thank God for giving me the opportunity to realize my dreams and to give me the force to continue even in the moments of adversity. I would like to thank my family and friends, especially my parents, Luis Torres and Elisa Chivara and my sister Erika Torres, for their unconditional love and support; I would never have done it without them.

Chapter 1 Introduction and Literature Review

Surfactants are a unique group of chemicals able to modulate interfacial properties. The importance of surfactants in surface modification lies in their self-association and self-assembly properties conferred by the presence of specific functional groups that lead to amphiphilic characteristics. The geometry and the stability of the surfactant structures are driven by the balance of van der Waals, hydrophobic, hydrogen-bonding and electrostatic interactions. Due to these forces, surfactants exhibit the *fluid-like* behaviors associated with colloids, complex fluids, and soft (structured) materials (1). Complex fluids are related to multi-component soft materials with non-Newtonian rheological behavior such as lipid membranes, cell suspensions and in general biological systems. Soft materials are systems easily deformed by forces including polymers, colloids, foams, liquid crystals and gels (2). Specific conditions in the solution such as the presence and concentration of electrolyte, the pH, the solvent and the nature of the interfaces direct the formation of aggregates. Micelles, vesicles, bilayers, monolayers, cylinders and other morphologies can be formed as a consequence of the intermolecular forces mentioned here (1). These last structures can be the components of soft materials and soft materials at interfaces.

Due to the molecular structure of surfactants consisting of functional groups with low attraction for the solvent (i.e. lyophobic or hydrophobic in water solutions) and a group with high attraction for the solvent (i.e. lyophilic or hydrophilic in water), surfactants can be oriented at interfaces. The lyophobic groups are mainly composed of aliphatic and aromatic

chains of different length and unsaturation degree, which confers an affinity for non-polar solvents or phases. According to the charge on the lyophilic group of the surfactant structure, surfactants can be classified as anionic, cationic, nonionic or zwitterionic. Most lyophilic functional groups undergo acid-base reactions leading to positive, negative or neutral charge. The electrostatic interactions arising from these charges then play an important role in determining the orientation and distribution of surfactants along an interface and their impact on the free energies of the interfacial area (3).

The pH dependence of surfactant properties has been an important subject of research because of its influence on micelle formation, modulating other properties such as solubility, interfacial tension, and rheological behavior of the phase that contains them and more specifically the interfacial area. Most of the ionic surfactants, such as soaps composed of fatty acids and salts, contain functional groups that are pH dependent. At a certain pH value, a solution containing pH-sensitive surfactant might exhibit a binary surfactant mixture between the protonated and deprotonated forms of the surfactant. Even although, at certain pH conditions one of the ionized or protonated monomer surfactant forms should predominate, the micelles formed may contain important quantities of both forms of the surfactants. Maeda et al. studied the surfactant dodecyldimethylamine oxide with an electrolyte concentration of 0.1 M NaCl and at pH 3, and they found that 1% of the surfactant monomer was ionized while 10% of the molecules forming the micelles are ionized (4, 5).

Within the forces responsible of adsorption of cationic surfactants on negatively charged surfaces, the Coulombic attractions are one of the most relevant. The ionic pair, formed

between the surfactant ion and the charged groups at the surface, trends to screen the surface charge density (6). Therefore, ionization of the surface groups increases because of the adsorption of ionic surfactant when increasing the pH. Goloub et al. studied the adsorption of the cationic surfactants (dodecylpyridinium chloride and cetylpyridinium) on silica, in the presence of KCl as an electrolyte. According to those studies, specific interactions between the cationic surfactants and the surface diminish when the number of charged sites at the surface increases because of an increase in salt concentration and pH values. Those findings suggest that the hydrophobic interactions between the aliphatic chains and the surface play an important role, as well as during surfactant aggregation at the silica/water interface (6, 7).

Because of the surface activity and self-assembly properties of surfactants, they have been widely used in a variety of applications including pulp and paper production, the food industry, paints, lacquers and plastics, mining, flotation and petroleum production, textiles and fibers, cosmetics and pharmaceuticals, agrochemicals, the leather and fur industry, as well as in detergents and cleaners (8). Due to the extensive use of surfactants, their release into the environment is ubiquitous. The environmental fate of these compounds is then determined in part by their interactions with mineral surfaces and natural organic matter found in soils.

The discharge of surfactants into sewage-treatments plants and as a consequence their dispersion into the environment and surface water effluents and sludges is ubiquitous. The surfactant toxic effects are determined in part by the final concentration reached in the aquatic medium and the degradation capacity through microbial activity. However, the biodegradation process products might bioaccumulate and their long-term effects require further studies (9).

In addition, Olkowska et al. presented evidence of surfactant contamination in different ecosystems under the influence of anthropogenic activities and how atmospheric deposition can eventually enable the migration of anionic, nonionic and cationic surfactants into the environment. According to those results, in regions considered to have low human activity, high quantities of surfactants were measured through monitoring of depositions such as run-off water, atmospheric precipitation, dew, and snow (10).

1.1 Cationic alkylammonium surfactants

Quaternary alkylammonium salts are a common type of cationic surfactant and are usually synthesized from either fatty acid or petrochemical sources (11), the positive charge arises from the nitrogen atom containing four alkyl substituents. An important property of this type of surfactant is the existence of a positive electric charge, which remains under acidic, neutral and alkaline conditions (3). Dodecyltrimethylammonium chloride (DTAC) is an alkylammonium surfactant with an aliphatic saturated chain of 12 carbons and three methyl substituents linked to the nitrogen atom **(Figure 1.1)**.

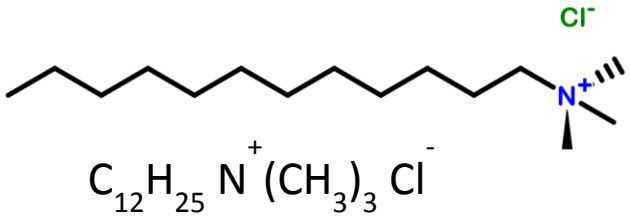

Figure 1.1 Molecular structure of dodecyltrimethylammonium chloride.

Previous studies have investigated the behavior of DTAC and its analogous bromide DTAB, in colloidal systems and the adsorption of cationic surfactants into environmental matrices (12, 13). Quaternary alkylammonium surfactants are often electrostatically attracted to natural

surfaces and materials, such as clays and (oxy)hydroxides, which typically contain an intrinsic negative charge. As a consequence, and depending on the surfactant concentration in the medium, the hydrophobicity of mineral interfaces in the environment is modified by surfactant adsorption, which leads to not only the retention of surfactants in the soil but also impacts the mobility of other xenobiotic substances, such as the polycyclic aromatic hydrocarbons (14).

DTAC and DTAB surfactants are used in Enhanced Oil Recovery operations (EOR). Salehi et al. performed a mechanistic study to describe the wettability alteration by DTAB adsorption to oil-wet carbonate rocks. According to those results, the cationic surfactant forms ionic pairs with the acidic components of crude oil. Once the ion-pair forms, the crude oil components adsorbed at the rock surface are removed, exposing the originally water-wet carbonate rock. These wettability changes are described in terms of imbibition where a wetting fluid (water) displaces a non-wetting fluid (oil) on the electrically charged rock surfaces. Thereby, fluids containing the cationic surfactant DTAB increase the recovery efficiency in surface carbonate rocks, due to oil displacement increasing the oil concentration in the fluidic phase recovered at the end of a hydraulic fracturing operation (15, 16). Therefore, the surfactant adsorption at the mineral surfaces in EOR is equally important to better understand the wettability changes at solid/liquid interfaces.

1.2 Silica surface properties

Although some studies regarding adsorption phenomena have elucidated the thermodynamics of how a solute interacts with a substrate under certain specific conditions (i.e. in an aqueous media and in the presence of electrolytes), there is a lack of information concerning how

changes in solvent structure and surface charge might direct solute adsorption. Such is the case for the silica surface when it is in contact with an aqueous medium at different pH values (17).

As previously stated, the interaction of mineral surfaces with cationic surfactants is charge dependent, where the pH of the solution plays an important role not only in determining surfactant ionization but the surface charge of minerals as well. In this section some properties of the silica surface are discussed. Silica is one of the most abundant mineral oxides in nature (18) and more specifically in sandstone oil reservoirs (19), which are often a target of EOR operations.

The bulk silica structure is formed by siloxane units joined in a tetrahedral lattice. At the surface, the identity and distribution of the functional groups present depends on the conditions used to treat the surface such as the temperature, and when the silica is in solution, the pH and the concentration of electrolytes. Particularly, acid/base reactions at the silica/water interface are fundamentally important because the relative concentrations of the neutral silanol (-SiOH) and the ionized sites ($-SiO^-$ or $SiOH_2^+$) determine the net surface charge, which influences the adsorption of other species such as metallic cations and cationic surfactants. Using second harmonic generation, a nonlinear optical technique sensitive to surface charge, Ong et al. determined the interfacial charge density at the silica/water interface for a range of pH values and obtained two pKa values for the silanol groups on the silica surface (20). According to this study, the first pKa was determined to be 4.5 and corresponded to 19% of the silanol sites whereas the second pKa was 8.5 and corresponded to the remaining 81% of the surface sites. Similarly, the experiments performed confirmed that the surface

potential is a function of pH with a maximum interfacial potential of 140 mV at pH 12 and in the presence of 0.5 M NaCl. On the other hand, at lower ionic strength the maximum surface potential was larger confirming that the presence of salt acts to screen the electrostatic field resulting from the negatively charged sites at the silica/water interface (20).

The presence of two pKa values for the silica surface is characteristic of a diprotic acid and those pKa values are associated with two different hydrogen bonding environments of the silanol sites (21). According to Ong et al., the isolated surface silanol groups correspond to the acidic pKa value (~ 4.5). The second pKa of 8.5 was attributed to silanols that are hydrogen bonded to neighbors (17, 22). In addition, Meties and co-workers have reported that 15 % of the silanol sites had a pKa of 5.5 whereas the remaining 85% have a pKa of 9.0, using potentiometric titrations measurements, which correlates with the results described previously by Ong et al (23).

The two pKa model proposed by Ong et al was based on experiments performed at high electrolyte concentration (0.5 M NaCl), but under low electrolyte concentration, the starting pH determines the number of the silanol sites observed. Darlington et al. established that at 0.01 M NaCl and starting at a pH value of 7, two detectable pKa values were observed at 3.8 ±0.1 and 8.6 ± 0.1. On the other hand, when starting the titration under alkaline conditions (pH 12), three pKa values were observed at 3.8 ± 0.3, 5.2 ± 0.5 and 9.6 ± 0.6. Furthermore, with a starting acidic pH value (pH 2) a slow SHG response was observed until a bulk pH of 4 and two pKa values of 5.3 ± 0.5 and 9.6 ± 0.6 were observed (21).

The pH value at which the net surface charge is equal to zero or the point of zero charge (PZC) of silica is between 2 and 4 (24). This means that at pH values lower than 2 the silica surface will be charged positively whereas at pH values higher than 4 the density of negatively charged sites is greater than the density of positively charged sites and thus the overall surface charge is negative (18). In this manner, the pH of the aqueous media determines the chemical nature of the substrate as well as the nature of the adsorbed compounds.

1.3 Adsorption of cationic surfactants at the silica/water interface

As mentioned above, the adsorption of charged species at the silica/water interface is pH dependent, because this parameter as well as the ionic strength of the solution will determine the electrostatic attraction between the surface sites and the charged adsorbates. Zhang and Somasundaran proposed a model to explain ionic surfactant adsorption on oppositely charged surfaces (25). It is named the Somasundaran-Fuerstenau model and it describes the interaction in four regions which are schematized in **figure 1.2**. The first region is characterized by the electrostatic adsorption of the charged head of the surfactant at the charged surface site, and this process is described by the Gouy-Chapman model, where the charge density is related with the electrostatic potential at the charged interface. In this region, the hydrocarbon chains of the surfactant do not have a preferential orientation and they might interact with hydrophobic sites at the surface. In the second region, when the surfactant concentration at the interface increases, the lateral interaction between the hydrocarbon chains increases leading to the formation of primary aggregates termed as hemimicelles (25). At this point of the isotherm, and because of the orientation of the hydrocarbon chains towards the bulk solution,

the surface is rendered hydrophobic or oil-wet. Evidence supporting this orientation of the hydrocarbon chains at this intermediate surfactant concentration has been presented by Hou et al. They performed contact angle and ζ potential experiments to study the adsorption of the cationic surfactant cetyltrimetylammonium bromide (CTAB) on a quartz surface at neutral pH. According to their results, there is an increase in the contact angle measurement resulting from a compact monolayer formed at the interface, which is accompanied by an increase in the ζ potential values (26).

In the third region of the Somasundaran-Fuerstenau adsorption isotherm, as the solution phase surfactant concentration increases, the adsorption mechanism is driven by the hydrophobic forces between the adjacent hydrocarbon chains rather than the electrostatic attraction between the head of the surfactant and the charged sites at the surface. At this surfactant concentration, the surface charge is near zero. Finally, in the fourth and last region of the isotherm, the surfactant monomer concentration in solution is approximately constant due to the monomer-micelle partitioning equilibrium and the adsorption density does not change because of the saturation of the surface with surfactant. The surfactant concentration at which the slope changes between the third and the fourth regions of the isotherm is approximately equal to the critical micelle concentration (CMC) of the surfactant. The CMC strongly depends on solution conditions such as the ionic strength, the pH, the temperature and the identity of the counter–ions present in the solution. When micelle formation takes place, the electrostatic repulsion between the charges on the surfactant molecules increases, but in the presence of electrolyte, the counter-ions decrease the repulsive interaction by screening the surfactant headgroup charge at the micelle surface allowing closer packing of the hydrocarbon chains. Velegol et al.

studied the effect of changing the identity of the counter-ion present in solution on surfactant interfacial structure by comparing CTAB with its analogous chloride CTAC. Atomic force microscopy images of CTAB and CTAC on silica showed that if the counter-ion is bromide and at a surfactant concentration 10 times the CMC, the aggregates are "worm-like" micelles adsorbed at the silica surface, whereas for CTAC at the same surfactant concentration the aggregates are circular projections (27). Hence the counter-ion clearly influences the size and the shape of the adsorbed aggregates.

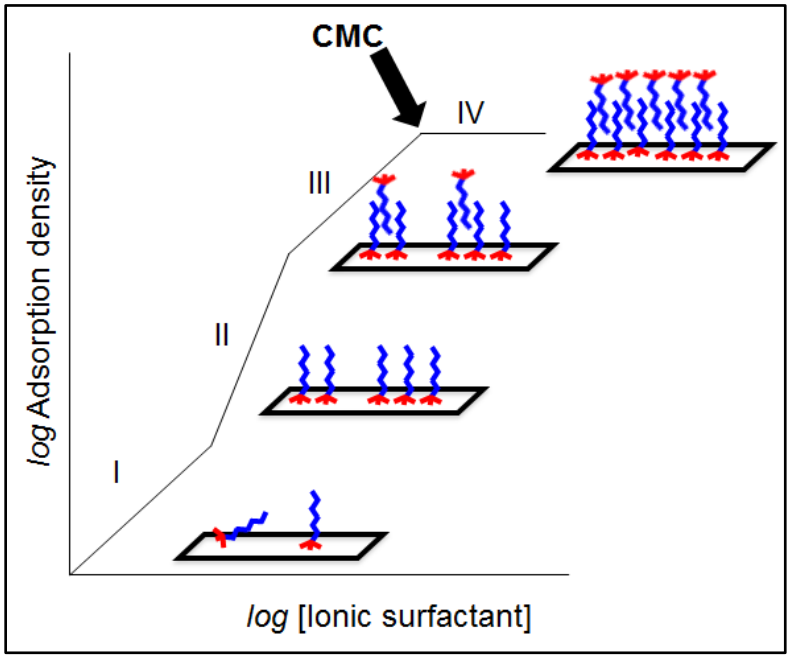

Figure 1.2 The four-region Somasundaran-Fuerstenau adsorption isotherm for ionic surfactants at charged surfaces. Further description in the main text.

Correlating the four region adsorption isotherm for ionic surfactants and in particular the third and fourth regions with experimental evidence, Hou et al. found that the contact angle decreases gradually in these regions for CTAB adsorbed on silica. This is attributed to the formation of a compact bilayer in which the hydrocarbon chains are buried in the adlayer and are not in direct contact with water rendering the surface more hydrophilic. ζ potential

measurements performed on the same system increased dramatically becoming more positive as the second layer of the aggregate facing the bulk solution was formed (26).

1.4 Sum Frequency Generation

Vibrational Sum Frequency Generation is a nonlinear optical spectroscopic technique with an inherent specificity to noncentrosymmetric systems used commonly to study surfaces and interfaces. To produce the SFG signal, two high energy laser beams, one with a fixed visible frequency ω_{VIS} and a tunable infrared beam ω_{IR}, are combined in time and space to produce a third beam which has a frequency that is the sum of the incident frequencies ($\omega_{SFG} = \omega_{VIS} + \omega_{IR}$). At non-charged interfaces, the SFG intensity is proportional to the square of the surface nonlinear susceptibility $\chi^{(2)}$ and the second order polarization $P_{SFG.}$

$$I_{SFG} \propto |P_{SFG}|^2 \propto \left|X_{NR}^{(2)} + \sum_v X_{R,v}^{(2)}\right|^2 E_{VIS}E_{IR} \qquad \text{Eq.1.1}$$

Where $\chi^{(2)}{}_{NR}$ and $\chi^{(2)}{}_{R}$ represent the nonresonant and resonant components or the second order susceptibility $\chi^{(2)}$, and E_{VIS} and E_{IR} are the electric fields generated by the visible and the infrared frequencies respectively (28, 29). The second order resonant susceptibility, $\chi^{(2)}{}_{R}$, is proportional to the number density of molecules, N, and the orientationally averaged polarizability $\langle\alpha^2\rangle$. This last term is presented in angular brackets to indicate the average of the molecular orientations at the interface (30).

$$\chi_R^{(2)} = N\langle\alpha\rangle \qquad \text{Eq. 1.2}$$

Thus, the square root of the SFG intensity is proportional to the density of molecules at the interface. The second order resonant susceptibility can be modeled as follows

$$\chi_R^{(2)} \alpha \sum_\nu \frac{A_\nu}{\omega_\nu - \omega_{IR} - i\Gamma_V} \quad \text{Eq 1.3}$$

Where A_ν is the amplitude of the vibrational mode ν, ω_ν is the resonant frequency, ω_{IR} is the IR frequency and Γ_ν is the line width of the transition (29). As it was stated before, SFG will be active only for molecules or vibrational modes without an inversion center, i.e. noncentrosymmetric systems. Previous studies of surfactant monolayers at interfaces (air/water (29), solid/water (31, 32), and oil/water (33)), have revealed that when the surfactant alkyl chains are in an *all-trans* conformation, they possess a local inversion center rendering the CH_2 stretches SFG inactive. If the conformation of the surfactant chain is locally noncentrosymmetric and forms what is known as a *gauche defect*, then the SFG vibrational modes become active. The ratio of the methylene and methyl stretches is therefore used as an indicator of the degree of conformational order in monolayers studied by SFG (29, 31, 34, 35).

At charged interfaces, there is a contribution from the third order polarization of the interface, which arises from the electrostatic field E_o.

$$P_{SFG} \alpha \chi^{(2)} E_{VIS} E_{IR} + \chi^{(3)} E_{VIS} E_{IR} \int_0^\infty E_0 \, dz \quad Eq. 1.4$$

The presence of this electrostatic field aligns the orientation of the water molecules in the interfacial region due to the strong permanent dipole in water, and accordingly the centrosymmetry of the interfacial region is reduced. Thus, this third order contribution to the SFG intensity increases when the interface is electrically charged, because the electrostatic field would align the interfacial water molecules resulting in a more significant contribution to the nonlinear polarization (29).

The study of molecular aggregation at interfaces is challenging in the sense that the techniques utilized should provide a sensitive and selective response that is able to differentiate the interfacial region from the bulk solution. Vibrational nonlinear spectroscopy techniques including Second Harmonic Generation (SHG) and SFG offer a powerful tool to describe interfacial phenomena due to their intrinsic specificity for noncentrosymmetric systems. One of the most important applications of surfactants lie in the petroleum industry where surfactants are used during the oil recovery process to change the wettability of mineral surfaces in sandstone reservoirs as well as the viscosity and permeability of the fluids containing the oil. The aim of this research project is to study the adsorption of a cationic surfactant, dodecyltrimethylammonium chloride (DTAC) at the silica/water interface with the spectroscopic technique Sum Frequency Generation over a range of pH varying from 3 to 11 and at a salt concentration pertinent to hydraulic fracturing fluids (100 mM NaCl).

Chapter 2 Article

The article presented in this chapter was submitted to publication on June 24th 2015 and published on September 23th 2015 in the *Journal of Physical Chemistry C.* The second author of this article, Mathilde Chaveau, was an intern during the summer of 2014. She developed the contact angle experiments as well as the interfacial tension measurements presented in the section 2.3.1. As first author, I performed the SFG experiments and wrote the article with the supervision of my research director Prof. Patrick L. Hayes. The article has been slightly modified in order to be compatible with the entire thesis.

DOI: 10.1021/acs.jpcc.5b06058

J. Phys. Chem. C 2015, 119, 23917−23927.

MACROMOLECULAR STRUCTURE OF DODECYLTRIMETHYLAMMONIUM CHLORIDE AT THE SILICA/WATER INTERFACE STUDIED BY SUM FREQUENCY GENERATION SPECTROSCOPY

L. Lorena Torres,† Mathilde Chauveau,‡ and Patrick L. Hayes*,†

†Department of Chemistry, Université de Montréal, 2900 Boulevard Édouard-Montpetit, Montreal, Quebec H3T 1J4, Canada.

‡Institute Universitaire de Technologie du Mans, Université du Maine, Avenue Olivier Messiaen, 72085 Le Mans, France.

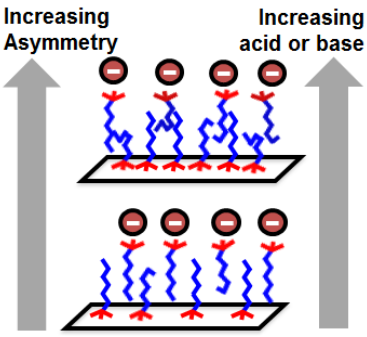

2.1 ABSTRACT

Adsorption of the cationic surfactant dodecyltrimethylammonium chloride at the silica/water interface was studied using sum frequency generation (SFG) spectroscopy under high ionic strength (100 mM NaCl) and at pH values ranging from 3 to 11, which are conditions relevant to hydraulic fracturing in enhanced oil recovery operations. At surfactant concentrations above the critical micelle concentration, SFG spectra of the CH stretching region indicate a more noncentrosymmetric structure for the surfactant aggregate is formed at the interface under acidic or basic conditions compared to neutral conditions. The SFG spectra also indicate a change in the packing/ordering of the surfactant hydrophobic tails with pH as well. In addition, the observed changes in the SFG spectra of water upon the addition of surfactant vary depending on the pH. At pH 7 and 11, the SFG intensity decreases in the OH stretching region, indicating a decrease in the magnitude of the electrostatic potential at the interface when the cationic surfactant is adsorbed at the negatively charged silica/water interface. At pH 3, an increase in the SFG intensity in the OH stretching region is attributed to an increase in the electrostatic potential at the silica/water interface due to the adsorption of a positively charged surfactant at a pH value close to the point of zero charge for the silica surface. These results demonstrate how the pH can influence the macromolecular structure of surfactants at mineral/water interfaces through the corresponding changes in the interfacial charge density and interfacial potential. In particular, we discuss how an unequal density of surfactants on each side of the interfacial bilayer or the adsorbed micelles may exist under either acidic or basic pH conditions.

2.2 INTRODUCTION

Surface modification using surfactants is pertinent to numerous commercial products and industrial processes, including pharmaceuticals, mineral ore flotation, pesticides, domestic hygiene products, and enhanced oil recovery (36-39). In these examples, surfactants are used to modulate interfacial properties such as wetting and colloidal stability (40). Quaternary ammonium surfactants are cationic amphiphilic compounds in which the nitrogen atom is charged positively, and these cationic surfactants are commonly used as wetting agents in a variety of technologies, including in enhanced oil recovery where they are an additive in hydraulic fracturing fluids (41). Thus, understanding the interactions of quaternary ammonium surfactants with mineral/water interfaces is fundamentally important for the optimization of hydraulic fracturing fluids and other technologies. For example, if surfactants irreversibly bind to mineral/water interfaces and cannot be recovered during a hydraulic fracturing project, then the cost of the project may be prohibitive (42). In addition, if the chemicals used in hydraulic fracturing are released into the environment (43), then their fate will be determined, in part, by interactions with environmental interfaces (12, 44).

Silica is one of the most abundant minerals in the earth's crust (18) and hydrocarbon reservoirs (19). When in contact with water, the silica surface has an intrinsic surface charge that depends on the bulk pH, with the surface silanol groups becoming negatively charged at pH values greater than the point of zero charge (PZC).

$$SiOH + H_2O \rightleftharpoons SiO^- + H_3O^+ \qquad \text{Eq. 2.1}$$

The PZC of the silica surface is generally located at pH values between 2 and 4 (24). According to nonresonant second harmonic generation studies of the silica/water interface performed by Ong et al., two pKa values (4.5 and 8.5) were found for the deprotonation of the silanol sites (20). The lower pKa value has been attributed to silanol groups associated with weakly hydrogen-bonded water, whereas the higher pKa value has been attributed to silanol groups associated with strongly hydrogen-bonded water (45). The relative surface concentration of these two sites depends on the electrolyte present in solution, but for NaCl, which is used in this study, the fraction of sites deprotonated at pH 7 is 20% (20, 45).

The influence of salt on the structure of water at mineral/water interfaces has been previously demonstrated in both experimental (46-48) and computational (49) studies. In general, the addition of salt leads to disruption of the hydrogen-bond network near the interface, and it also screens the static electric field from the charged silica surface. This screening leads to a shorter Debye length, which defines the depth of penetration of the static electric field into the adjacent aqueous solution. In the context of this study, the addition of salt also impacts the macromolecular structure of ionic surfactants by reducing the critical micelle concentration (CMC) via screening of the repulsion between the surfactant headgroups.

In the limiting case of very low surfactant concentrations, adsorption of a cationic surfactant on silica occurs due to the Coulombic attraction between the surfactant headgroups and the silica surface sites (31). As a consequence, the net surface charge will decrease and the hydrophobicity will increase. Once a certain concentration of surfactant is reached, aggregates

form (50). Different measurement techniques have been used to constrain the possible macromolecular structures of surfactant aggregates at solid/liquid interfaces, including atomic force microscopy (27) and neutron scattering (51). In addition, the nonlinear optical technique sum frequency generation (SFG) spectroscopy has emerged as an important method for characterizing surfactant adsorption due to its sensitivity to the symmetry of the surfactant aggregation (e.g., monolayer versus bilayer), and its surface specificity, which allows the vibrational spectrum of the interfacial species to be measured.

Although previous papers have described the macromolecular structure of cationic surfactants on silica at concentrations near the CMC,(27, 31) there is a lack of research investigating how the pH changes the aggregate structure in which techniques such as SFG are used to directly probe the surfactant at the solid/liquid interface. The pH is an important parameter in many different surfactant-containing technologies, including enhanced oil recovery (52), which potentially could alter the macromolecular structure of adsorbed surfactants through electrostatic interactions. Indeed, two previous studies of alkylammonium surfactant adsorption on silica, one at pH 11 and the other under neutral conditions (pH ≈ 5.5), exhibited very different SFG spectra in the C−H stretching region (31, 53). Under basic conditions, C−H resonances were observed, indicating the formation of asymmetric aggregates, whereas, under neutral conditions, no such resonances were observed, which indicates the formation of symmetric aggregates. While the pH and the corresponding differences in the silica surface charge are a plausible explanation for the observed differences, it is not possible to make a confident conclusion regarding the role of the pH because there are other differences between

the two studies that are confounding variables (i.e., the ionic strength and counterions present in solution).

To address this unresolved question, the adsorption of the alkylammonium surfactant dodecyltrimethylammonium chloride (DTAC) at the fused silica/water interface is systematically studied here over a range of pH values using SFG for the first time (to our knowledge). In addition, contact angle and interfacial tension measurements are used as a complement to the SFG experiments. Experiments are carried out at high ionic strength (0.1 M NaCl) because surfactant-containing hydraulic fracturing fluids often contain high concentrations of salt, and it has been well demonstrated by the papers discussed in the Introduction that the addition of salt can change the water structure in the interfacial region as well as influence surfactant aggregation. Furthermore, the addition of a background electrolyte minimizes the change in ionic strength when the pH is adjusted, allowing the effect of the pH to be better separated from the effect of the changing ionic strength.

Ultimately, the goal of this work is to better characterize the pH-dependent adsorption and macromolecular structure of surfactants at interfaces, which until now had not been systematically investigated using SFG spectroscopy. The interfacial macromolecular structure is fundamentally linked to the amount of surfactant adsorbed and the wettability of a surface, both of which are important to optimizing surfactant-based technologies (42, 54). In addition, the structure of water in the interfacial region is investigated, which has important implications for mineral reactivity, including dissolution and adsorption (44).

2.3 EXPERIMENTAL SECTION

2.3.1. Contact Angle and Interfacial Tension Measurements. A First Ten Angstroms (FTA 200) flexible video system was used to measure sessile contact angles on fused silica slides (Chemglass, CGQ-0640-01), as well as the interfacial tension via the pendant drop method. The slides were cleaned following the same procedure used for the fused silica windows analyzed in the SFG experiments, and this procedure is described in the next subsection. The CMC at different pH values and in the presence of 100 mM NaCl was determined from the interfacial tension measurements as discussed in section 2.4.1.

2.3.2. Materials and Reagents. The DTAC solutions (Sigma-Aldrich, 99.0+%) were prepared in Millipore water (18.2 MΩ cm at 25 °C, TOC (total organic carbon) ≤ 3 ppb) or D_2O (CDN Isotopes, 99.9 atom % D), and the pH or pD was adjusted with NaOH (Sigma-Aldrich, 99.99%), NaOD (Sigma-Aldrich, 40 wt % in D_2O, 99.5 atom % D), HCl (EMD, Omni Trace), and DCl (Sigma-Aldrich, 35 wt % in D_2O, 99 atom % D) solutions. For the deuterated surfactant experiments, DTAB-d_{25} (dodecyl-d_{25}-trimethylammonium bromide; CDN Isotopes, 99.1 atom % D) was used. NaCl (Merck, 99.5%) was used to prepare the solutions with added salt. Prior to each experiment, an IR-grade fused silica window (ISP Optics, QI-W-38-3) and the slides for contact angle measurements were cleaned by being rinsed with Millipore water and then HPLC-grade methanol. The window and the slides were then dried at 100 °C for 2 h and plasma cleaned for 5 min at 400−800 mTorr of oxygen. It should be noted that there are some minor compositional differences between normal and IR-grade fused silica, most importantly the reduced concentration of hydroxyl ion in the IR-grade fused silica. However,

in the presence of water, both silica surfaces are generally expected to terminate in hydroxyl groups, which can be protonated or deprotonated (45, 55).

A thin film of PMMA (poly(methyl methacrylate); MW 35000, Acros Organics) was deposited onto an IR-grade fused silica window, and the SFG spectrum at the silica/air interface was collected before and after each DTAC experiment. The maximum of the SFG peak corresponding to the CH symmetric stretch of the methoxy group in the polymer, which is nominally located at 2955 cm^{-1}, was used to calibrate the frequency. The same experimental geometry and alignment were used for this calibration and the DTAC studies (53, 56). The DTAC solutions were contained in a custom-built Teflon reservoir, and the IR-grade fused silica window was clamped on the open top of the reservoir and sealed with a Viton O ring. Before the DTAC experiments, the sample cell was rinsed three times with the solution containing the surfactant. Aqueous DTAC, or DTAB-d_{25}, solutions were introduced into the reservoir using a pipet and allowed to equilibrate for 20 min. All the experiments, including the SFG experiments, were carried out in duplicate to verify the reproducibility of the experiments.

The pH of each solution was adjusted with dilute solutions of NaOH and HCl or with their deuterated analogues, and the pH was measured with a pH meter (Orion Star A121, Thermo Scientific). The solutions were prepared and the pH was adjusted the day before the experiments were carried out to allow for equilibration with ambient CO_2. For multiple samples spanning the range of pH values used here, the pH value was verified after the samples were allowed to sit overnight in sealed bottles. In general, the change in pH was

negligible compared to the broad range of pH values used in these experiments and less than 0.5, indicating that CO_2 dissolution did not substantially alter the pH of the samples.

2.3.3. SFG Spectroscopy. SFG spectroscopy is a nonlinear optical technique that allows the measurement of vibrational spectra with a high level of interfacial specificity. In the SFG experiment, two pulsed laser beams are overlapped on a sample, a visible beam with frequency ω_{vis} and an infrared beam with tunable frequency ω_{IR}, producing a third beam with a frequency that is the sum of the incident frequencies ($\omega_{SFG} = \omega_{vis} + \omega_{IR}$). The vibrational spectrum is measured by tuning the IR frequency and measuring the SFG intensity, which is enhanced when the IR frequency approaches the vibrational resonances of a molecule at the interface (35, 57). At an uncharged interface, the intensity of the emitted SFG light (I_{SFG}) is proportional to the second-order nonlinear susceptibility of the interface ($\chi^{(2)}$). However, for charged interfaces, such as the silica/water interface at pH values not equal to the PZC, the SFG intensity will also contain a contribution from the third-order susceptibility ($\chi^{(3)}$) (46, 47). The total SFG intensity can then be expressed as

$$I_{SFG} \alpha \left|\chi^{(2)} E_{vis} E_{IR} + \chi^{(3)} E_{vis} E_{IR} \int_0^\infty E_0(z) dz\right|^2 \quad \text{Eq. 2.2}$$

where E_{vis} and E_{IR} are the visible and IR electric fields, E_0 is the static electric field, and z is the distance normal to the interface. Furthermore, the second- and third-order susceptibilities are proportional to the number of molecules at the interface (*N*) and to the second- and third-order polarizabilities ($\langle\alpha^{(2)}\rangle$ and $\langle\alpha^{(3)}\rangle$). The angular brackets in the equation below indicate that the polarizabilities are averaged over the molecular orientations (30):

$$\chi^{(2)} = N^{(2)}\langle\alpha^{(2)}\rangle,\ \chi^{(3)} = N^{(3)}\langle\alpha^{(3)}\rangle \quad \text{Eq. 2.3}$$

Within the electric dipole approximation, $\langle\alpha^{(2)}\rangle$ is nonzero only in noncentrosymmetric and ordered environments, whereas $\langle\alpha^{(3)}\rangle$ is nonzero in isotropic environments and increases in magnitude in ordered noncentrosymmetric environments (47).

For the silica/water interface, only the interfacial region is noncentrosymmetric, and the second-order contribution is therefore inherently interface specific due to anisotropic forces that lead to polar alignment of molecules. With respect to the third-order contribution, in principle, the interface specificity of this contribution is defined by the penetration depth of E_0 into the aqueous phase. The Debye length is a metric for this depth, and for the high ionic strengths used in this study (i.e., 100 mM NaCl), it is equal to ~1 nm. Therefore, the SFG spectrum of the charged interface which arises from both the second- and third-order polarizations will be highly selective for the interfacial region.

As shown in the following equation, SFG spectra are often modeled using a constant nonresonant background and a serie of Lorentzian functions for the frequency-dependent resonant response (30).

$$I_{SFG}(\omega_{IR}) = \left|A_{NR} + \sum_{\nu}\frac{A_{\nu}}{\omega_{\nu} - \omega_{IR} - i\Gamma_{\nu}}\right|^2 \qquad \text{Eq. 2.4}$$

Here, A_{NR} is the amplitude of the nonresonant contribution, A_ν and ω_ν represent the amplitude and the frequency of the resonant mode ν, and Γ_ν is a damping constant. While Eq 2.4 does not explicitly account for the second- and third-order contributions to the SFG spectrum, the nonresonant and resonant terms could arise from the second- and/or third-order polarization.

The scanning SFG system (EKSLPA) consists of a PL2241 series picosecond laser that generates fundamental (1064 nm) and second harmonic (532 nm) beams that pump a PG501/ DFG parametric generator, which produces an IR beam that was tuned from 2700 to 3850 cm^{-1}. The 532 nm and tunable IR lasers were directed through an IR-grade fused silica window and overlapped in time and space at the solid/liquid interface with incident angles of 49° and 55° from the surface normal (after refraction) for the visible and IR beams, respectively. The generated SFG signal is isolated using optical filters and a monochromator and is then detected by a photomultiplier tube. All SFG spectra are measured by monitoring the s-polarized SFG field generated by s-polarized visible light and p-polarized IR light. SFG spectra were collected with acquisition times ranging between 1 and 2 h per spectrum. The SFG data for each spectrum were normalized by dividing the SFG intensity at each wavelength by the product of the visible and infrared energies, which were monitored during the experiments using calibrated photodiodes and beam splitters.

2.4 RESULTS AND DISCUSSION

2.4.1. Contact Angle and Interfacial Tension Measurements. Figure 2.1a presents contact angle measurements on fused silica slides at pH 3, 7, and 11 with 100 mM NaCl. For all three pH values, at low surfactant concentration, the contact angle increases until a DTAC concentration of about 2 mM. According to Young's equation (58), this trend indicates the adsorption of a hydrophobic monolayer of surfactant beyond the contact line, which decreases the interfacial tension at the silica/air interface, and/or the formation of hydrophobic domains at the silica/water interface, which increases the interfacial tension at this interface. Once the

maximum value for the contact angle is reached, the contact angle decreases to 15° asymptotically. This result is consistent with the formation of a bilayer (i.e., an extended planar bilayer or packed adsorbed micelles) at high surfactant concentrations, since much higher contact angles would be expected if the hydrophobic tail of the surfactant were exposed to the water (59).

Previous work on cetyltrimethylammonium bromide (CTAB)-an alkylammonium surfactant with a hydrophobic chain that is four carbons longer than that of DTAC-using ζ potential measurements as well as ellipsometry has suggested that at a certain concentration a surfactant monolayer forms at the silica/water interfaces due to electrostatically driven adsorption (26). The hydrophobic chains of the surfactant molecules in the monolayer are exposed to the aqueous phase, leading to the observed increase in the contact angle. When the concentration of surfactant continues to increase, a compact bilayer may be formed with the hydrophilic headgroup now pointed toward the aqueous phase, which leads to a decrease in the contact angle. However, this proposed explanation for the change in wettability does not agree with an earlier study that indicates CTAB only forms centrosymmetric macromolecular structures at the silica/water interface (31). The reasons for this difference are not entirely clear, although both studies agree that bilayers exist at high surface coverage. Ultimately, it is difficult to infer the structure at the solid/liquid interface using only the contact angle data presented here due to the well-known fact that the interfacial tensions for the solid/liquid and solid/air interfaces cannot be independently quantified. SFG measurements can help to resolve this uncertainty.

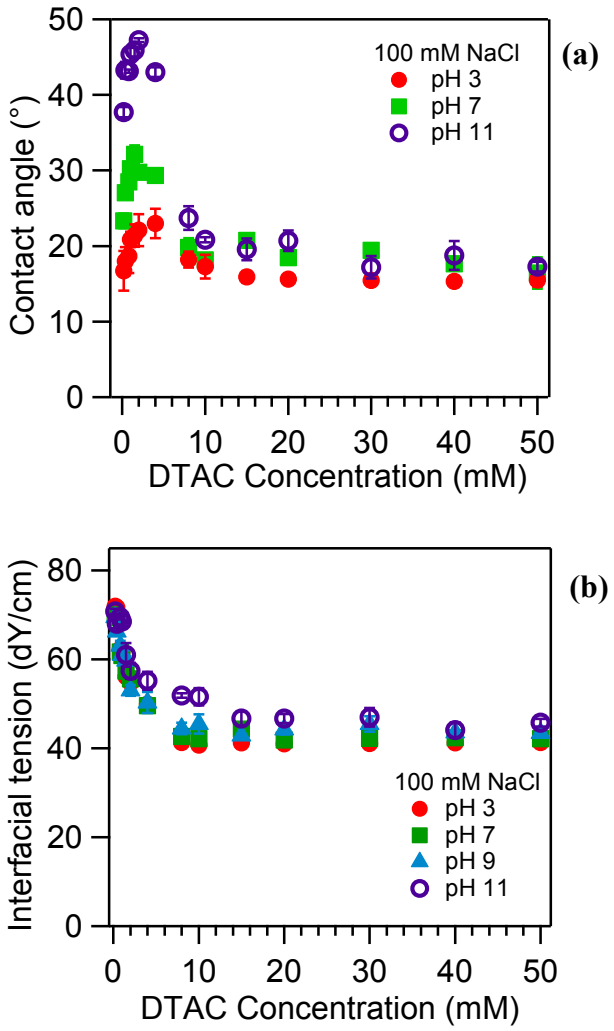

Figure 2.1 (a) Sessile contact angle measurements as a function of the bulk DTAC concentration with 100 mM NaCl on a quartz surface. (b) Interfacial tension at the solution/air interface determined by the pendant drop method.

Differences in the contact angle at acidic, neutral, and basic pH are observed below approximately 10 mM DTAC. Surfactant adsorption is influenced by several different types of interactions such as surfactant−surface electrostatic attraction as well as surfactant−water hydrophobic interactions. At pH 3, which is near the PZC, surfactant adsorption on the silica surface will be less favorable due to the reduced electrostatic attraction. Increasing the pH leads to higher negative surface charge density, which likely results in increased surfactant

adsorption due to the greater extent of surfactant− surface electrostatic interactions (60). Thus, at basic pH, the increased surfactant adsorption at the silica surface may be responsible for higher contact angles than observed at acidic and neutral pH values. However, at surfactant concentrations greater than 10 mM, the interface is saturated or nearly saturated with surfactant at all pH values, and thus, there is no change in contact angle with the pH. This reasoning is consistent with a previous optical reflectometry study on cetylpyridinium bromide that measured an increase in surfactant adsorption with increasing pH at low surface coverages but no change in the amount of adsorbed surfactant with increasing pH at high surface coverages (61).

Interfacial tension measurements were also performed on DTAC solutions with 100 mM NaCl at pH 3, 7, 9, and 11 (Figure 2.1b). For a given pH value, the CMC corresponds to the concentration at which the interfacial tension ceases to decrease with increasing surfactant concentration. Thus, the CMC at pH 3, 7, and 9 is 7 mM, whereas at pH 11 the CMC is 14 mM. To obtain these values, the data in Figure 2.1b were interpolated according to the method described by Rehfeld et al (62). The quaternary ammonium on the surfactant headgroup is positively charged regardless of the pH, and also the change in ionic strength with the pH is negligible due to the addition of 100 mM NaCl. Thus, the difference in the CMC at pH 11 relative to the more acidic pH values must be due to other factors. One possible explanation is the presence of OH^- ions that adsorb to the surface of micelles and displace chloride ions. It is known that the identities of the counterions can influence the CMC of alkylammonium surfactants (27), although it is not possible to conclude definitively from the interfacial tension measurements that OH^- adsorption is responsible for the change in CMC with the pH. Rather,

further experiments with a greater range of salt/OH^- concentrations are needed using surfactant that has been recrystallized to remove trace impurities (e.g., amines which exhibit acid/base chemistry).

2.4.2. SFG Spectra of Adsorbed Surfactant. SFG experiments were carried out to characterize the interfacial vibrational spectrum of DTAC in the CH stretching region as a function of pD. These experiments for the CH stretching region were performed in D_2O to avoid overlapping between the CH and OH resonances of water. Figure 2.2 presents the SFG spectra collected at different pD values in the presence of 100 mM NaCl using 15 mM DTAC. The concentration of DTAC was selected to ensure that all experiments were performed at a concentration above the CMC and where the contact angles did not exhibit a dependence on the pH. The SFG spectra were collected starting at a pD of 7, and then the pD was either increased or decreased until a pD of 3 or 11 was obtained. In both cases, the CH resonances exhibit a minimum in relative intensity at pD 7, and the intensity increases as the DTAC solution becomes more acidic or more basic. A similar trend was also observed for experiments carried out at a DTAC concentration of 10 mM that will be included in a future paper that examines the SFG spectra as a function of the DTAC concentration. The increase in the SFG intensity with the addition of base is consistent with a study carried out by Tyrode et al (31) at near-neutral conditions where CH resonances were not observed for CTAB adsorbed at the silica/water interface in which the lack of peaks was attributed to the centrosymmetric structure of the aggregate, as well as a later study by Hayes et al (53) carried out at pH 11 that observed CH peaks in the SFG spectra for the same surfactant and interface. The SFG spectra

shown in Figure 2.2 indicate that the surfactant macromolecular structure at the silica/water interface becomes more noncentrosymmetric with the addition of acid or base.

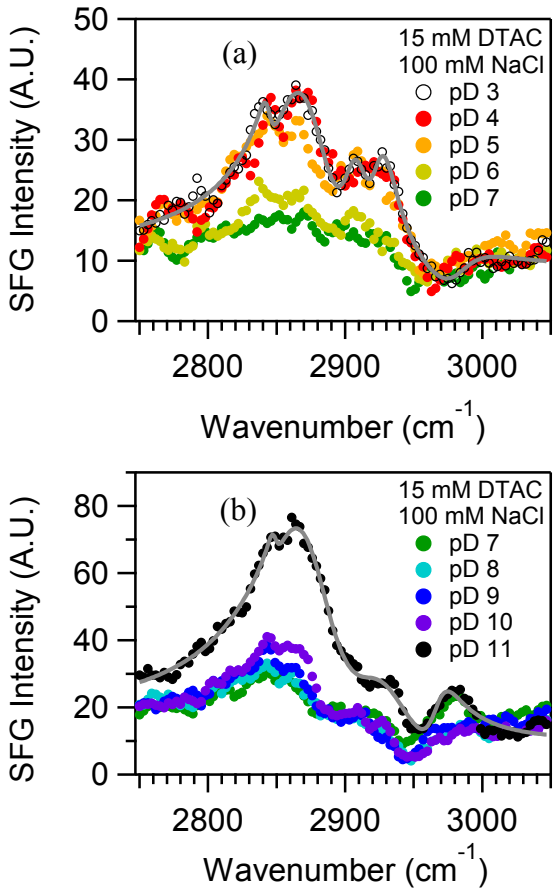

Figure 2.2 SFG spectra in the CH stretching region for the surfactant DTAC adsorbed at the silica/D_2O interface as a function of the pD. The conditions for the experimental results shown in each panel are the following: (a) 15 mM DTAC and pD 3−7 and (b) 15 mM DTAC and pD 7−11. The solid lines indicate fits of eq 2.4 to the data using the peak assignments in Table 2.1 and the parameters summarized in Tables 2.2 and 2.3.

To analyze the SFG spectra in more detail, the peaks were assigned to CH stretching modes as summarized in Table 2.1 using the spectra at pD 3 and 11 that exhibited the best signal-to-noise ratios. The peak assignment was facilitated by comparing SFG spectra for DTAC and DTAB-d_{25} as shown in Figure 2.3. For DTAB-d_{25}, which contains CH_3 groups on the

quaternary ammonium headgroup but a deuterated tail, only one very weak peak was observed at ~2970 cm^{-1}, which indicates that the peaks appearing at lower wavenumbers are due to the methyl and methylene groups on the surfactant tail. For the DTAC spectra, the peaks observed

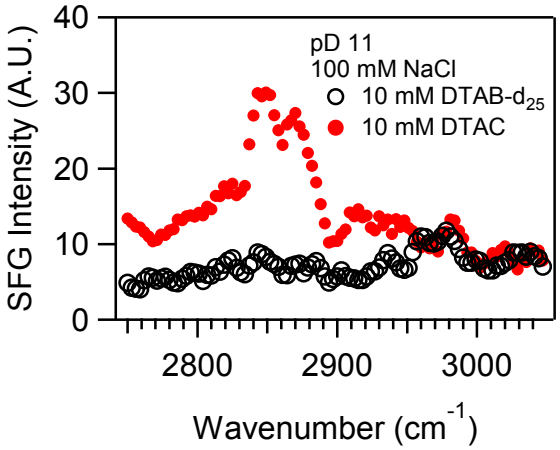

Figure 2.3 SFG spectra for DTAB-d_{25} and DTAC in the presence of 100 mM NaCl and at pD 11. The spectra were collected at the silica/ D_2O interface. The weak peak at ~2970 cm−1 in the spectrum of DTAB-d25 is attributed to the methyl asymmetric stretch for the surfactant headgroup.

at 2967 cm^{-1} (pD 3) and 2982 cm^{-1} (pD 11) are thus attributed to the methyl symmetric stretch for the surfactant headgroup (31). Then the SFG peaks observed at ~2845 and 2876 cm^{-1} are assigned to the symmetric vibrational modes of the methylene and methyl groups of the surfactant tail, respectively. Continuing with the peak assignment, Fermi resonances of the symmetric stretches of the methylene and methyl groups of the tail were observed at 2907 and 2925 cm^{-1}, respectively. The resonances found in the range between 2907 and 2982 cm^{-1} exhibit low intensities and low signal-to-noise ratios compared to the symmetric stretches, and therefore, the assignments of these resonances are relatively uncertain. In addition, whereas the methyl groups bonded directly to the nitrogen atom are spectroscopically resolved, there is no distinct peak for the methylene group adjacent to the nitrogen. The lack of distinct spectral features for this methylene could be due to the combination of both low SFG signals and small

shifts in the frequency of the vibrational resonances relative to the other methylene groups on the hydrophobic tail of the surfactant.

Table 2.1 Assignments for the CH Stretching modes of adsorbed DTAC (28, 31, 35, 53, 56).

Designation	Mode	Wavenumber (cm^{-1}) (pD3, pD11)
d^+	CH_2 symmetric stretch	2844, 2849
r^+	CH_3 symmetric stretch	2876,2876
d^+_{FR}	CH_2 symmetric stretch (Fermi resonance)	2907, no peak
r^+_{FR}	CH_3 symmetric stretch (Fermi resonance)	2925, 2924
r^+_{HG}	CH_3 symmetric stretch of the headgroup	2967, 2982

Focusing on the symmetric modes, the SFG spectra were fitted with Eq 2.4 in the range between 2750 and 2890 cm^{-1} to determine the amplitude of these modes. The results are presented in Figure 2.4. For the experiments from pD 7 to pD 11 (Figure 2.4b), the amplitudes for the methylene and methyl symmetric stretches increase with the pD, although the increase in the methyl symmetric stretch amplitude is within the estimated uncertainties of the fit. The observed trend is nevertheless consistent with an increasingly noncentrosymmetric macromolecular structure for the surfactant aggregate with respect to the surface plane (29, 31, 35, 63). Therefore, a possible explanation for the increase in the amplitude of the methylene and methyl stretches is an increasingly unequal density of surfactant molecules between the side of the bilayer (or adsorbed micelles) directed toward the aqueous phase and the side directed toward the silica.

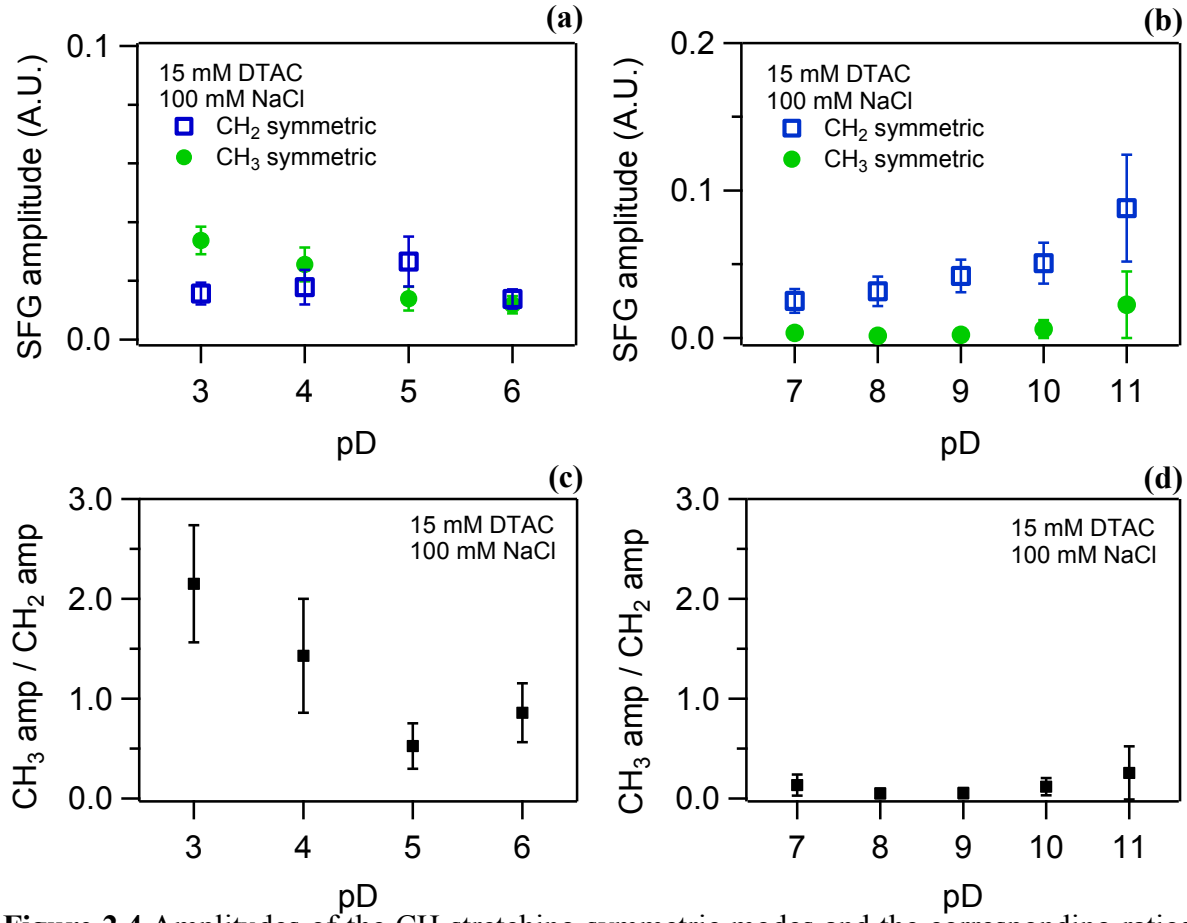

Figure 2.4 Amplitudes of the CH stretching symmetric modes and the corresponding ratios of the amplitudes (CH_3/CH_2). Data are plotted as a function of the pD. The amplitudes were obtained using eq 2.4 to fit the spectra in Figure 2.2. Fits were carried out for the spectral range between 2750 and 2890 cm−1. The data displayed and the corresponding conditions for each panel are the following: (a) amplitudes between pD 3 and pD 6, (b) amplitudes between pD 7 and pD 11, (c) ratios between pD 3 and pD 6, and (d) ratios between pD 7 and pD 11. For panels a and c, the results at pH 7 are not presented because the signal-to-noise ratios of the CH resonances were not sufficient to accurately fit the data. Panels c and d are plotted on the same vertical scale to facilitate comparison of the results.

It is known that when the surfactant is in an *all-trans* conformation at an interface, the more symmetric structure results in a weaker methylene intensity in the SFG spectrum compared to the case where the chains contain gauche defects. The difference in intensity is due to the oppositely oriented oscillators in the *all-trans* conformation leading to SFG contributions that destructively interfere. Therefore, the ratio of the methyl to methylene amplitudes can be used

as a qualitative indicator of the number of gauche defects (33, 34, 64). Within the uncertainties of this analysis, this ratio does not change between pD 7 and pD 11 (Figure 2.4d), which indicates that there is not a significant change in the packing of the surfactant tails. This result is consistent with the hypothesis given above that the increase in the SFG amplitudes is due to an unequal density of surfactants on each side of the aggregate rather than, for example, an increase in the number of gauche defects.

In Figure 2.4a, the trends for the methylene and methyl symmetric stretches when increasing the acidity are somewhat different from those for increasing basicity. While the amplitude for the methyl group on the hydrophobic tail seems to increase, the amplitude of the methylene group in this pD range exhibits no trend. In addition, the ratio of the amplitudes (CH_3/CH_2) generally increases, although not for each pD step, indicating a reduction in the number of gauche defects when the pD is lowered to 3. If an unequal density of surfactant molecules in the two sides of the aggregate were to exist under acidic conditions, similar to that proposed for basic conditions, then the resulting increase in the methylene amplitude may be offset by the concurrent reduction in the number of gauche defects, which would explain the lack of an increasing or decreasing trend for the methylene amplitude.

In general, when comparing neutral, acidic, and basic conditions (Figure 2.4c,d), the ratios indicate a higher incidence of gauche defects at neutral and basic pH and so a more disordered conformation of the surfactant at the silica/water interface. Another possible way that the conformation could be become more disordered is through the stronger interaction with the silica surface at neutral and basic pH, which results in a different conformation for the CH_2

groups near the headgroup in the proximal leaflet compared to those in the distal leaflet of the bilayer. This asymmetry would increase the CH_2 amplitude in the SFG spectra in a manner similar to a gauche defect. Regardless of the exact molecular origin of the more disordered conformation, it appears that the relatively strong electrostatic interaction between the silica and surfactant at neutral and basic pH distorts the structure of the aggregate possibly due to the roughness of the fused silica surface on the molecular scale.

2.4.3. SFG Spectra of Water in the Presence of DTAC. In addition to carrying out SFG measurements in the CH stretching region, SFG spectra of water (2700−3850 cm^{-1}) were collected as a function of the pH, NaCl concentration, and surfactant concentration to better understand how the electrostatic potential and charge varies at the interface. It has been previously established that the intensity of the SFG spectrum of water is sensitive to the electrostatic field created by surface-bound charges, because the electrostatic field gives rise to a third-order contribution to the SFG intensity as discussed above. In general, the intensity of the water spectrum is strongly correlated with the magnitude of the electrostatic field and charge density at the interface (46, 47, 49). Therefore, by analyzing the overall intensity for the SFG spectrum of water, one can obtain a qualitative measure of the surface change and interfacial potential for the silica/water system studied in this work.

Figure 2.5 presents the SFG spectra for the silica/water interface at pH 3, 7, and 11 with added DTAC surfactant.

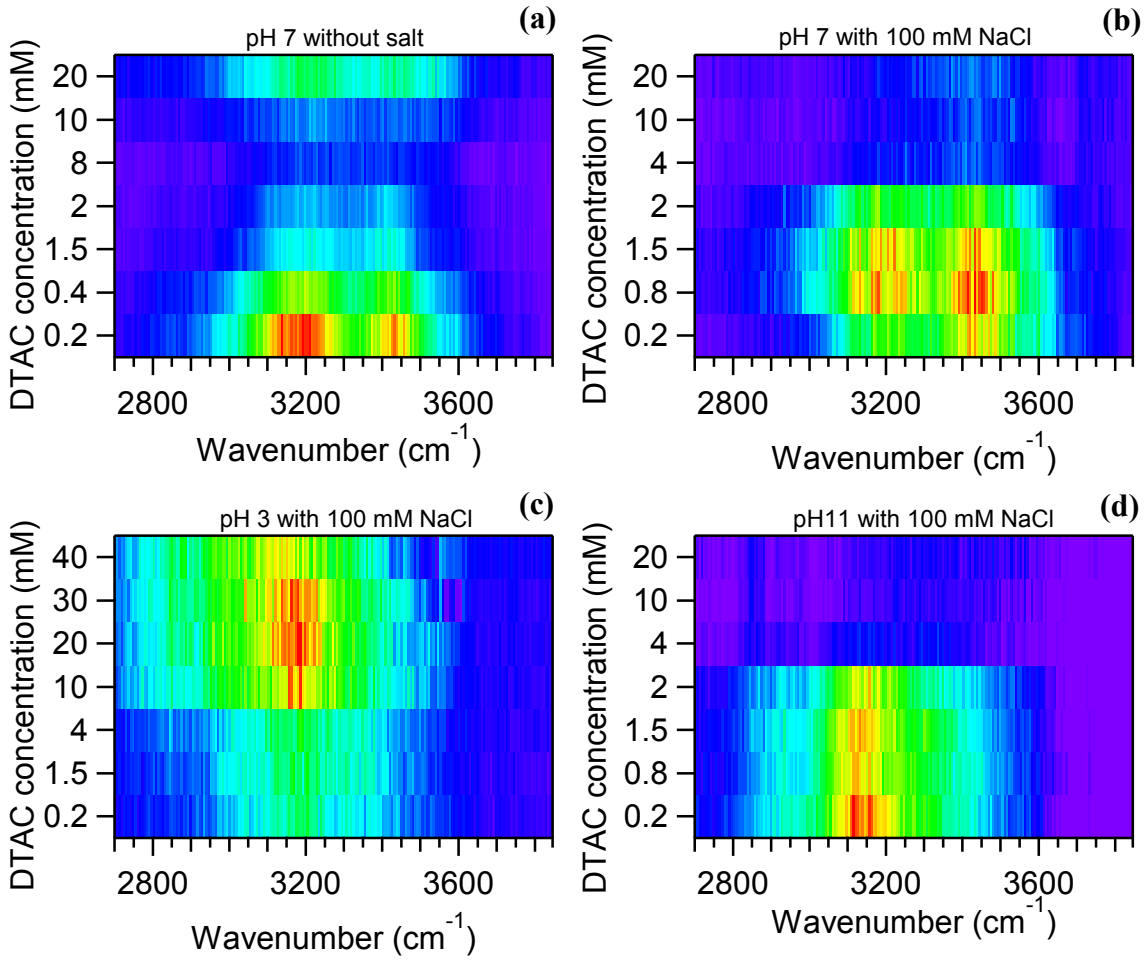

Figure 2.5 SFG spectra in the CH and OH stretching regions for DTAC at three different pH values: (a) pH 7 without salt, (b) pH 7 with 100 mM NaCl, (c) pH 3 with 100 mM NaCl, and (d) pH 11 with 100 mM NaCl. The spectra were collected at the silica/H_2O interface. Note that the spectra are presented as image plots in which the DTAC concentration axis is not scaled linearly. Instead the concentrations for the SFG experiments were selected to sample the different regions in the contact angle and interfacial tension measurements, while also considering the relatively lengthy SFG acquisition times.

Specifically, Figure 2.5a shows the SFG spectra for DTAC concentrations ranging between 0.2 and 20 mM at pH 7 without addition of salt, which exhibit two OH stretching resonances at ~3200 and ~3450 cm^{-1}. These peaks have been attributed previously to strongly and weakly hydrogen-bonded water (48, 65), and while these peaks can provide important insight into the structure of water at interfaces, for this study we rather focus on the overall intensity

of the water spectrum. Thus, it is noted that the spectra at pH 7 without added salt show a clear trend of decreasing and then increasing intensity with the surfactant concentration. The decrease in SFG intensity can be explained by the decrease in the electrostatic field that penetrates into the solution when the negative charge of the silica surface is compensated for by the positively charged surfactant. (This decrease may also be due to the displacement of water molecules from the interface.) At higher concentrations, there is charge overcompensation where the interface becomes positively charged due to an excess of adsorbed surfactant. In previous work, the minimum in the SFG signal has been used to estimate the surfactant concentration at which the net surface charge is zero (31), and this concentration is ~8 mM DTAC. Recent work by Hou et al (26) on CTAB adsorption to quartz has shown behavior similar to that observed here for neutral pH conditions without added salt. Specifically, in that work the ζ potential was originally negative, and this potential was neutralized at an intermediate surfactant surface density. As the concentration of the surfactant was increased further, the ζ potential became positive, indicating overcharging due to adsorption. These findings are entirely consistent with the SFG spectra described in this paragraph.

In Figure 2.5b, the concentration range and the pH are the same as those used in Figure 2.5a, but the spectra were collected in the presence of salt (100 mM NaCl). Similar to the experiment without salt, the SFG intensity decreases at DTAC concentrations near 4 mM, but in contrast, the SFG intensity does not recover at the highest surfactant concentrations studied here. This difference can be explained by increased chloride adsorption to the aggregate, which balances the positive interfacial charge from the adsorbed surfactant. This conclusion is

consistent with a previous second harmonic generation study of CTAB adsorption to silica under high ionic strength conditions (10−500 mM NaCl), which found extensive chloride coadsorption within the aggregates and determined that the ratio of surfactant molecules to chloride is approximately 4:3 (56). Thus, taking into account the results presented here as well as this previous study, at the highest surfactant concentrations and in the presence of 100 mM NaCl, the sum of the charge from the silica, surfactant, and chloride at the interface is near zero, which means that the $\chi^{(3)}$ contribution due to the static electric field is relatively weak.

Figure 2.5c shows the analogous results for pH 3 and 100 mM NaCl. For this pH the opposite trend is observed compared to that for pH 7. At low surfactant concentrations, the SFG signal remains constant, but at concentrations greater than 4 mM, the SFG intensity increases until 30 mM with a subsequent decrease at the highest concentration, 40 mM. This behavior is consistent with the fact that, at pH 3, near the PZC, the silica surface is neutral or has a very low charge density. As surfactant concentrations are increased, aggregate formation still occurs at the interface despite weak electrostatic interactions. If the positive charge of the aggregates is not fully balanced by coadsorbed chloride, then the resulting positive electrostatic field would lead to the increase in SFG intensity that is observed in Figure 2.5c. The decrease in SFG intensity between 30 and 40 mM DTAC may be due to the high surfactant concentration relative to the added NaCl. At this concentration, it is expected that the surface is saturated or nearly saturated with surfactant on the basis of the contact angle measurements as well as the measured CMC. Thus, the increase in the bulk surfactant concentration does not substantially increase the interfacial charge density. However, the added surfactant and chloride in solution still screen the static electric field and thereby

decrease the $\chi^{(3)}$ contribution to the SFG intensity. A similar increasing trend followed by a decrease due to the competing effects of the surface charge density and electrostatic screening was observed by Covert et al. for the CaF_2/water and poly(methyl methacrylate)/water interfaces (46).

Lastly, the SFG spectra were also collected at pH 11 with 100 mM NaCl for concentrations of surfactant between 0.2 and 20 mM (Figure 2.5d). At low bulk surfactant concentrations, the SFG signal remains unchanged until 1.5 mM DTAC, but at concentrations above this value, the signal decreases and remains low at the highest DTAC concentrations studied. The trend in the SFG intensity is the same compared to that for the experiments at pH 7 with 100 mM NaCl, although the negative silica surface charge density is higher at basic pH. The static electric field due to the silica surface which gives rise to the $\chi^{(3)}$ contribution is reduced by adsorption of surfactant, but overcompensation of the negative surface does not occur. To determine if overcompensation of the silica surface charge is possible without added salt for pH 11, an SFG experiment was carried out under these conditions (*data not shown*). The trend in the intensity of the OH resonances is nearly identical to that observed for the experiment with 100 mM NaCl. The similar trends with and without added NaCl at pH 11 suggest that an excess of chloride is not needed to balance the positive charge due to the surfactant aggregate. Rather the deprotonated silanol sites, adsorbed chloride from dissolved DTAC, and/or adsorbed hydroxyl ions are sufficient to balance the positive charge.

The relative intensity of the two peaks in the water SFG spectra has been used previously as an indicator of changes in the water coordination, and a shift in intensity from 3200 to 3450

cm^{-1} has been attributed to disruption of the hydrogen-bonding network (46). Focusing on the SFG spectra for the highest surfactant concentrations with 100 mM NaCl, for pH 3 the intensity maximum is at ~3200 cm^{-1}, whereas the spectra at pH 7 and 11 have greater intensity near 3450 cm^{-1} (as indicated by the blue and cyan regions). These differences indicate that water at the surfactant-containing silica/water interface is more ordered at pH 3 versus pH 7 and 11, which is consistent with the conclusion that the interface is charged at pH 3 and neutral or weakly charged at pH 7 and 11. The charged interface at pH 3 maintains the hydrogen-bonding network, despite the presence of added surfactant and salt, which acts to disrupt this network at pH 7 and 11. The differences in solvent structure have important implications for the reactivity of the surfactant-containing silica/water interface and can influence processes such as binding of coadsorbates as well as mineral dissolution (48, 66).

Returning to the subject of the increase in the CMC concentration at pH 11, previous work at the air/water interface observed a change in the relative SFG intensity at 3200 and 3450 cm^{-1} for increasing concentrations of NaOH (67), but the microscopic explanation for why the presence of OH^- in the interfacial region alters the SFG spectrum has been controversial. Changes in the SFG spectrum have been attributed to an excess of OH^- at the interface (68). However, recent modeling work has alternatively attributed these changes to two phenomena: (1) the formation of a buried electrical double layer in which the Na^+ is slightly more buried at the interface and (2) the solvation of OH^- (69). Clearly, it is difficult to make a definitive conclusion on whether OH^- is adsorbed at the interface without molecular dynamics simulations and also without the use of heterodyne detection of the SFG spectra (70), and such work is outside the scope of this current paper.

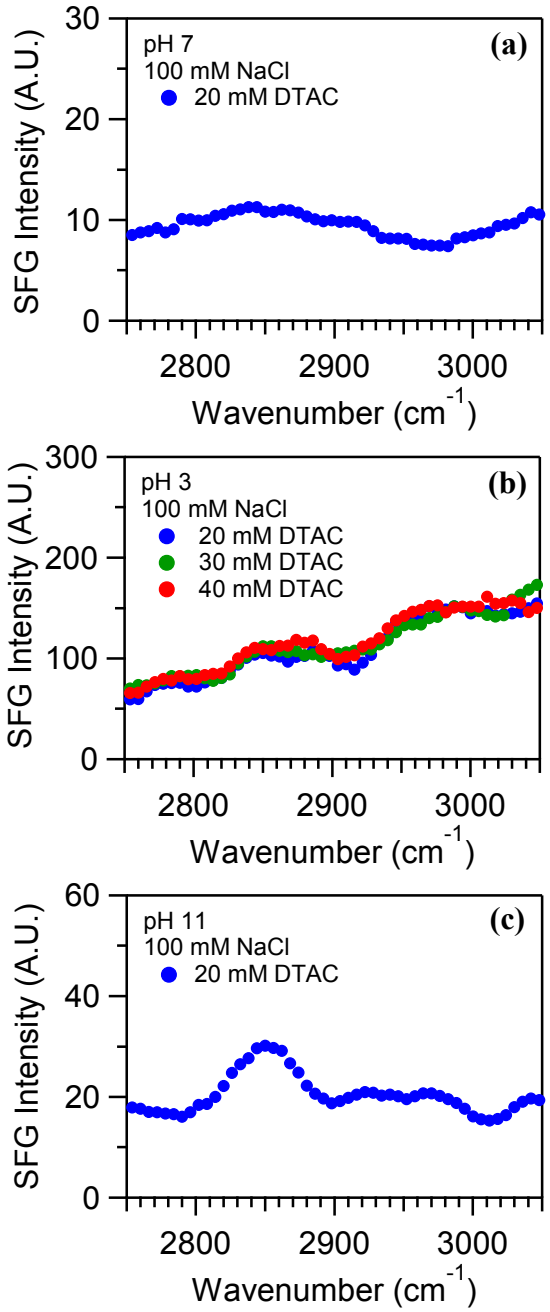

Figure 2.6 SFG spectra in the CH stretching region for high surfactant concentrations in the presence of 100 mM NaCl at (a) pH 7, (b) pH 3, and (c) pH 11. The spectra were collected at the silica/H_2O interface.

Importantly, the SFG spectra of DTAC at the silica/H_2O interface in the presence of 100 mM NaCl exhibit CH stretching modes as also observed in the experiments with D_2O. In Figure

2.6, the spectra for the CH stretching region are shown for the experiments with H_2O. For pH 7, the peaks are relatively weak for the methyl and methylene groups of the surfactant at 20 mM DTAC, but these peaks are more prominent at pH 11, which is qualitatively similar to the result with D_2O (Figure 2.2b). Once again, these results suggest the macromolecular structure of the surfactant becomes more noncentrosymmetric with the addition of base.

The same comparison between pH 7 and pH 3 is more difficult due to the strong interference at pH 3 between the CH resonances and the shoulder of the OH resonances, which are very intense. Given that SFG is a coherent spectroscopy, the CH and OH contributions to the spectra can constructively or destructively interfere with each other, and quantifying the CH amplitudes requires careful deconvolution of this interference. Such interference effects may also explain why at pH 11 and pD 11 the SFG signal is 2 times higher when D_2O is used instead of H_2O. Even under basic conditions and in the presence of 20 mM DTAC and 100 mM NaCl, there is still significant intensity in the OH stretching region that overlaps with the CH stretches (although the difference in CH peak intensity could also simply be due to small changes in the timing and alignment of the IR and visible lasers, since the data in Figures 2.2 and 2.6 were collected on different days). As demonstrated above, we have ultimately chosen to carry out the SFG experiments in D_2O to reduce the interference with the OH resonances.

2.5 CONCLUSIONS

Even though it is not possible to infer the exact aggregate structure formed at the silica/water interface by the adsorbed DTAC, SFG spectroscopy probes the changes in the symmetry of

the aggregate in a way that is not possible with other surface analysis techniques. While using D_2O to better quantify peak amplitudes in the CH stretching region, an increase in the amplitudes for the CH symmetric stretches is observed when the pH increases from 7 to 11 or decreases from 7 to 3 for surfactant concentrations above the CMC. These trends in the SFG spectra with the pH indicate that a more noncentrosymmetric aggregate is formed under acidic or basic conditions.

For the SFG spectra of water in the presence of 100 mM NaCl, the change in the water spectral intensity with increasing DTAC concentration is different at pH 3, 7, and 11. At pH 7 and 11, the overall SFG intensity decreases with added DTAC. This result can be explained by the decrease in the electrostatic field at the silica/water interface when the positive DTAC adsorbs to the negatively charged silica, which will decrease the third-order contribution to the SFG spectrum. In contrast, at pH 3 the SFG intensity increases with added DTAC, which is consistent with an increase in the electrostatic field due to positively charged surfactant adsorbing at an interface that is not strongly charged.

We propose the following explanation for the observed changes in the aggregate symmetry with the pH; this explanation is also summarized in Figure 2.7. For this figure it has been assumed that the adsorbed surfactant forms a bilayer; however, the same logic presented below applies if adsorbed micelles were formed instead. (We note that SFG is insensitive to transitions between these two different morphologies since they are both centrosymmetric.) Regarding other possible morphologies of the surfactant aggregate, the formation of wormlike micelles is unlikely given that previous studies of cetyltrimethylammonium, a C16

alkylammonium surfactant, observe the formation of wormlike micelles only at NaCl concentrations that are at least 5 times higher than the concentrations used in this work (56, 71). In addition, given previous X-ray reflectometry and neutron reflection measurements, it is unlikely that a substantial amount of the surfactant adsorbs to the silica surface with its hydrophobic chain when the surface density of the surfactant is high (72, 73). For the pH values between 7 and 11, it is well-known that the silica surface becomes increasingly negatively charged due to deprotonation of silanol groups. This increase in charge makes adsorption more favorable on the side of the aggregate facing the silica surface relative to the side facing the aqueous solution. The distribution of surfactant molecules between the two sides of the aggregate is then increasingly noncentrosymmetric with increasing pH, giving rise to a more intense SFG spectrum in the CH stretching region. With decreasing pH from 7 to 3, the silica surface becomes neutral since the PZC is between pH 2 and pH 4. The density of the surfactant on the side of the aggregate facing the aqueous solution will be relatively low compared to that on the side facing the silica, because the silica and surfactant directly adsorbed to the silica will form a plane of positive charge that makes adsorption less favorable on the opposite side of the aggregate due to electrostatic repulsion. Some of the positive charge at the interface due to adsorbed surfactant will be offset by chloride that is coadsorbed, but the increasing intensity of the water resonances with the DTAC concentration at pH 3 indicates that this coadsorption is not sufficient to completely neutralize the positive charge from the surfactant.

In addition, using the ratio of the methyl to methylene symmetric stretch amplitudes, it is possible to infer how the ordering of the surfactant tails changes as a function of the pH. Between pH 7 and pH 11, there is no significant change in the ordering despite the increasing

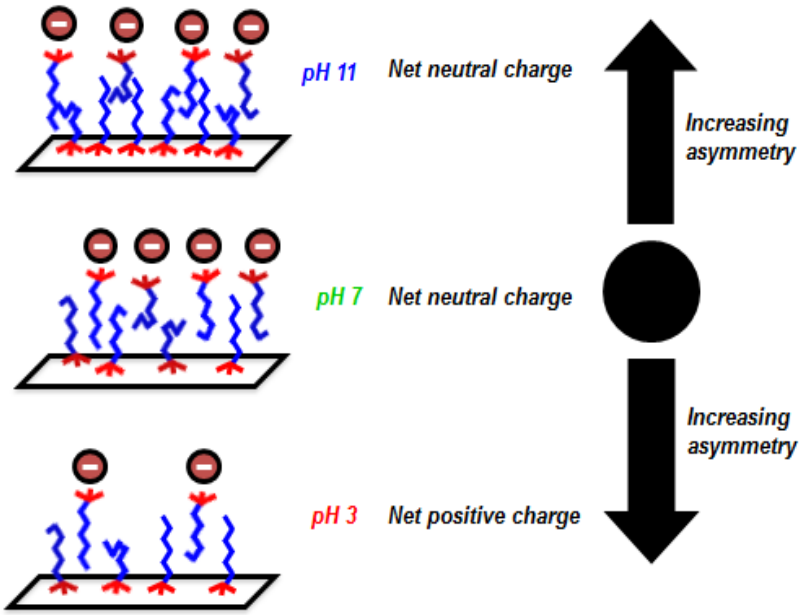

Figure 2.7 Proposed changes in the macromolecular structure of DTAC at the silica/water interface, which are induced by acidic or basic pH conditions. These changes are inferred from experiments carried out in 100 mM NaCl and at high surfactant surface coverages. At both pH 3 and pH 11, experiments suggest that the surfactant densities on the two sides of the aggregate are not equal (i.e., the density is higher on the side of the aggregate adjacent to the silica surface). The spheres with negative charge indicate the coadsorbed counterions (e.g., chloride).

amplitude of the methyl and methylene symmetric stretches. A different trend is observed under acidic conditions where the spectra at pH 3 indicate the methylene groups are in a more symmetric environment, which may be due to a reduction in the number of gauche defects at pH 3 compared to pH 7.

From the SFG results described here, it is clear that the bulk pH can influence the macromolecular structure of surfactants at the silica/water interface. It is noted that even though this study has focused on adsorption to mineral/water interfaces under conditions relevant to hydraulic fracturing, including high ionic strength, the same phenomenon is relevant to other systems as well where there is a difference in electrostatic potential across an aggregate of amphiphilic molecules. For example, the adsorption of charged species to biological membranes is important in a variety of biological processes, and recent work has demonstrated that the attractive electrostatic interactions between a polypeptide and a phospholipid bilayer are sufficient to induce an asymmetric structure in the supported bilayer (74). Thus, electrostatically driven changes in macromolecular structure at interfaces may be important for a variety of environmental, industrial, and biological processes.

2.6 ACKNOWLEDGMENTS

Engineering Research Council of Canada (NSERC) Discovery Grant (RGPIN/05002-2014), the Canada Foundation for Innovation (CFI; Project Number 32277), and the Université de Montréal. L.L.T. acknowledges a scholarship from the Faculté des études supérieures et postdoctorales de l'Université de Montréal. We also thank Professor Paula Wood-Adams for generously providing access to Concordia University's SFG system.

2.7 SUPPORTING INFORMATION

Table 2.2 Parameters obtained from Figure 2.2 after fitting the spectra at pD 3 using Equation 2.4. The fittings and uncertainties (one standard deviation) were calculated using the software package IGOR Pro v6.3.4.0.

Designation	Mode	ω_ν (cm^{-1})	A_ν	Γ_ν
d^+	CH_2 symmetric stretch	2844 ± 1	0.004 ± 0.002	6 ± 2
r^+	CH_3 symmetric stretch	2876 ± 1	0.24 ± 0.03	32 ± 3
d^+_{FR}	CH_2 symmetric stretch (Fermi resonance)	2907 ± 1	0.04 ± 0.02	13 ± 3
r^+_{FR}	CH_3 symmetric stretch (Fermi resonance)	2925 ± 1	0.04 ± 0.02	12 ± 3
r^+_{HG}	CH_3 symmetric stretch of head-group	2982 ± 2	0.03 ± 0.01	23 ± 6

Table 2.3 Parameters obtained from Figure 2.2 after fitting the spectra at pD 11 using Equation 2.4. The fittings and uncertainties (one standard deviation) were calculated using the software package IGOR Pro v6.3.4.0.

Designation	Mode	ω_ν (cm^{-1})	A_ν	Γ_ν
d^+	CH_2 symmetric stretch	2849±1	0.002 ± 0.001	4 ± 3
r^+	CH_3 symmetric stretch	2876±1	0.33 ± 0.05	35 ± 3
r^+_{FR}	CH_3 symmetric stretch (Fermi resonance)	2924±1	0.14 ± 0.04	30 ± 4
r^+_{HG}	CH_3 symmetric stretch of head-group	2967±1	0.03 ± 0.01	13 ± 2

Chapter 3 Additional experiments

The results in this section are complementary to the results presented in the article "Macromolecular Structure of Dodecyltrimethylammonium Chloride at the Silica/Water Interface Studied by Sum frequency Generation Spectroscopy" presented in Chapter 2 of this thesis. Calibration of the wavenumber scale for the SFG experiments and additional information regarding the adsorption of DTAC surfactant under acidic and alkaline conditions are discussed in this chapter. Finally, experiments in the OH region of the SFG spectra are presented to support the findings in Section 2.4.3.

3.1 SFG spectrum of the polymer Poly(methyl methacrylate), PMMA, at the silica/air interface

In order to monitor the stability of the SFG signal during the experiments, the SFG spectrum of the polymer PMMA was collected at the beginning as well as at the end of a set of experiments. Another important reason for measuring the SFG PMMA spectrum is to calibrate the wavenumber scale at a single point. A thin layer of PMMA was drop cast onto a flat IR grade fused silica window. The window was previously cleaned according to the procedure described in Section 2.3.2 (Materials and Reagents). A solution of PMMA at a concentration of 2 wt % (prepared in HPLC-grade Acetone) was dried at room temperature onto the IR grade fused silica window. Once the solvent had been evaporated, the SFG spectrum of PMMA was collected by placing the window on the custom-built Teflon reservoir so that the laser beam

passed through the window before focusing on the PMMA surface. The first SFG spectrum of PMMA was collected after aligning the laser system and verifying the measured signal was due to SFG rather than scattered light from either the VIS or IR beams. Immediately after the last SFG spectrum is collected at the fused silica/water interface, the reservoir is dried carefully and the window containing the PMMA film is mounted on the reservoir, and a second PMMA spectrum is collected. The SFG spectra of PMMA were collected in a range from 2900 cm^{-1} to 3000 cm^{-1}. A clear and distinct peak in the SFG signal must be observed between 2945 and 2955 cm^{-1}, which corresponds to the CH symmetric stretch of the methoxy group in the polymer (75), to confirm that the stability and the quality of the SFG signal was sufficient during the SFG experiments.

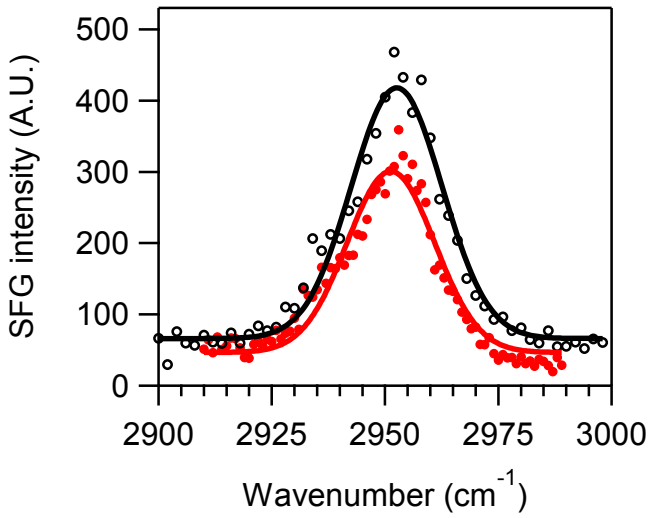

Figure 3.1 SFG spectra of PMMA at the PMMA/air interface, at the beginning (red circles) and at the end (black empty circles) of a set of DTAC experiments. The solid lines are the fits using a Gaussian function with a maximum peak value at 2951 and 2953 cm^{-1} for the collected spectrum at the beginning and at the end of the experiment, respectively.

Figure 3.1 presents two PMMA spectra collected at the beginning (red circles) and at the end (black empty circles) of a set of DTAC experiments. According to these results, there is no

significant change in the wavenumber value where the stretch for the methoxy group of the PMMA polymer is observed. The SFG PMMA spectrum indicates thus that the SFG system is functioning properly and there is no major misalignment of the Vis and IR lasers. In the case where there is a serious misalignment of the SFG system, no peak would be observed at 2955 cm^{-1}. In addition, if the peak is not near 2955 cm^{-1}, then it is probable that there is a problem with the calibration of the wavenumber.

3.2 CH stretching resonances of the surfactant DTAC at the silica/D_2O interface

According to the SFG spectra collected at different pH values and DTAC concentrations (Chapter 2, Figure 2.5), SFG intensity increases in the CH stretching region of the spectra (between 2700 and 3050 cm^{-1}) at pH 3 and pH 11 when increasing the DTAC bulk concentration. At this point it is important to note that because of the overlapping between the CH and the OH resonances in the SFG spectrum, it was necessary to use a deuterated solvent (D_2O) in order to eliminate this interference from the SFG spectrum of the surfactant adsorbed at the silica/water interface. For the results presented in this section as well as those of section 2.4.2, the pD was adjusted using an Orion Star pH meter with a gel-filled epoxy-body pH/ATC electrode. Experiments using glass electrodes (76) to measure pH and pD have observed a correction factor of +0.4. This correction factor is negligible in this study since the pH was adjusted in steps of 1.

The SFG experiments were then carried out specifically in the CH stretching region in a wavenumber range from 2750 to 3050 cm^{-1}. Figure 3.2a presents the results at pD 3 with 100

mM NaCl with DTAC concentrations ranging from 0.2 to 40 mM. According to these results, the SFG intensity increases with increasing DTAC concentration at concentrations near and above the CMC. (The CMC is 7 mM at pH 3 in the presence of 100 mM NaCl as presented in Section 2.4.1). This increase can be attributed to two factors: (1) the centrosymmetry of the DTAC aggregate adsorbed at the fused silica surface is disrupted and the adsorbed structure has a more noncentrosymmetric distribution of aliphatic chains, or (2) that the interfacial density of the surfactant is increasing even at concentrations above CMC, due to direct adsorption of micelles.

A similar trend is observed at pD 11 both in the absence and in the presence of NaCl (Figure 3.2b and c). The SFG intensity increases when increasing the DTAC bulk concentration suggesting a more noncentrosymmetric structure of the surfactant at the interface. For all the spectra presented in the CH region and when using D_2O (Figures 2.2, 2.3, and 3.2), the symmetric stretches for the methylene and the methyl groups have a higher SFG intensity compared with the stretches at wavenumbers above 2900 cm^{-1}.

Regarding the peak assignment in the CH stretching region of the SFG spectra, the peaks at 2845 ± 10 cm^{-1} and 2875 ± 10 cm^{-1} correspond to the symmetric stretches for the methylene and methyl groups respectively (**Tables 2.1 and 3.1**). For the peak assignments between 2900 and 3000 cm^{-1} the poor signal-to-noise ratio makes it more difficult to identify the different vibrational modes of the surfactant at the silica/D_2O interface. Thus, our study and analysis are centered on the symmetric stretches. Despite this challenge, an important peak was observed at approximately 2970 cm^{-1}. This peak is attributed to the CH symmetric stretch of the methyl

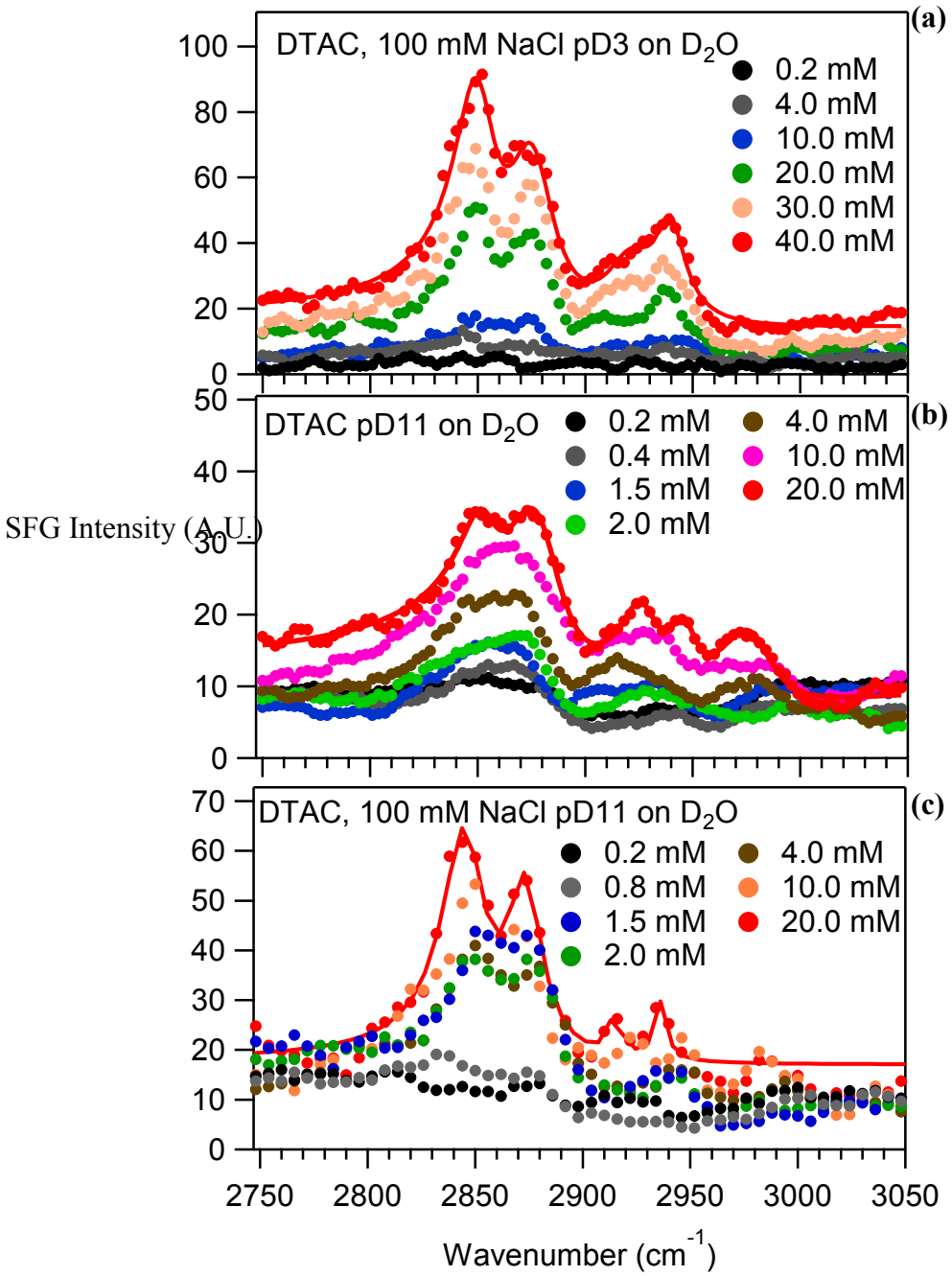

Figure 3.2 SFG spectra in the CH stretching region for the surfactant DTAC at the silica/D_2O interface as a function of DTAC concentration. (a) DTAC with 100 mM NaCl at pD 3, (b) DTAC without the addition of salt at pD 11 and (c) DTAC with 100 mM NaCl at pD 11. The solid lines represent the fits using Equation 2.4 at the highest concentrations for the same set of spectra.

group linked to the quaternary amine. The assignment of this peak was facilitated by the SFG spectra comparison of the deuterated surfactant DTAB-d_{25} and DTAC according to the results

(Figure 2.3) already discussed in Chapter 2. Moreover, this assignment is consistent with the Raman spectra presented by Tyrode et al. for CTAB (31).

The peak assignments for the Fermi resonances of the symmetric stretches (2915 ± 15 cm^{-1} and 2925 ± 20 cm^{-1} for the Fermi resonances of the methylene and methyl symmetric stretches, respectively) are uncertain. In order to fully analyze the identity of the different peaks observed in the range between 2900 and 3000 cm^{-1}, a study involving different polarization combinations and selective deuteration of the surfactant is required. Importantly, since the deuterated analogs are not commercially available, the synthesis of those compounds would be required.

Table 3.1 Assignments for the CH stretching modes of adsorbed DTAC on silica. The results correspond to the SFG spectra displayed in Figure 3.2.

Assignment	**Mode**	**ω_v (cm^{-1}) pD 3 100 mM NaCl 40 mM DTAC**	**ω_v (cm^{-1}) pD 11 without NaCl 20 mM DTAC**	**ω_v (cm^{-1}) pD 11, 100 mM NaCl 20 mM DTAC**
d^+	CH_2 symmetric stretch	2851 ± 1	2854 ± 1	2846 ± 2
r^+	CH_3 symmetric stretch	2876 ± 1	2880 ± 1	2873 ± 3
d^+_{FR}	CH_2 symmetric stretch (Fermi resonance)	2922 ± 3	2928 ± 1	2915 ± 10
r^+_{FR}	CH_3 symmetric stretch (Fermi resonance)	2940 ± 1	2947 ± 1	2936 ± 6
r^+_{HG}	CH_3 symmetric stretch of the headgroup	No peak	2978 ± 1	No peak

Continuing with the analysis of the methylene and methyl symmetric stretches observed at pD 3 and pD 11 and shown in Figure 3.2, the square root of the normalized SFG intensity as a function of the DTAC concentration is presented in Figure 3.3. The square root of the SFG

intensity in the CH region is equal to the SFG electric field, E_{SFG}, and it is used as an indicator of the density of surfactant adsorbed at the silica/D_2O interface, if one assumes there is no change in the centrosymmetry of the adsorbed surfactant. The data points at pD 11 have a similar behavior with and without addition of 100 mM NaCl. Initially, the E_{SFG} increases with increasing DTAC concentration until 10 mM. After this surfactant concentration, between 10 and 20 mM of DTAC, the E_{SFG} is constant suggesting that the maximum surface coverage is reached and this observation is supported by the contact angle measurements (Figure 2.1a).

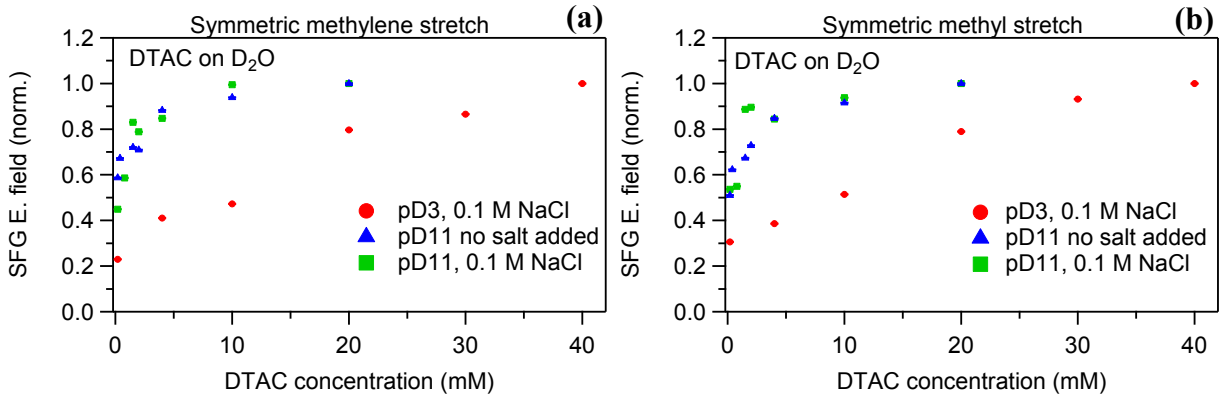

Figure 3.3 Normalized SFG Electric field corresponding to the symmetric methylene **(a)** and methyl **(b)** stretches as a function of surfactant concentration. Red circles are data at pD 3 containing 0.1 M NaCl; blue triangles are data at pD 11 without addition of salt and green squares are data at pD 11 with 0.1 M NaCl. Uncertainties were estimated based on the standard deviation of the SFG intensity for seven wavenumbers selected from the baseline region (between 2770 and 2790 cm^{-1}) for each spectrum collected under the same alignment and experimental conditions, e.g. the same pD and the presence or absence of salt. Since the estimated uncertainties are relatively low, those values are indicated by the size of the marker for each point presented on the graph.

The surfactant surface coverage may not be the same with and without the addition of salt, because the chloride anion decreases the electrostatic repulsion between the positively charged surfactants in the adlayer at the silica/D_2O interface. However, the presence of a strong negative surface charge may also reduce this electrostatic repulsion thus the addition of NaCl

may not have as strong an effect on the adsorbed surfactant density compared to less basic conditions. The increasing trend in SFG intensity is observed for the methylene (Figure 3.3a) and the methyl (Figure 3.3b) symmetric stretches, although there is a slight difference when comparing the relative intensity for the methyl symmetric stretch for the systems with and without added NaCl. This difference can be attributed to the different orientations of the methyl group with respect to the plane of the silica surface leading to a more noncentrosymmetric distribution of the methyl group at 100 mM NaCl.

Regarding the results at pD 3 with 100 mM NaCl, the trend is different compared to the results presented for pD 11. The increase in SFG electric field is more gradual because of the low charge density of the silica surface at pD 3, which makes less favorable the electrostatic interactions between the surfactant and the silica surface. In spite of the weak electrostatic interactions, surfactant adsorption still occurs and it is directed by the hydrophobic forces of the adjacent aliphatic chains of DTAC (77). Given the range of the DTAC concentration tested at pD 3, it is expected that the saturation of the silica surface will be reached at higher DTAC concentrations than those studied here due to the absence of a flat region in Figure 3.3, as was observed at pD 11. Nevertheless, the overall amount of adsorbed surfactant might change very little at higher concentrations, and the change in the SFG intensity can be large because of differences in the packing and conformation of the surfactant under acidic conditions.

3.3 SFG spectra of water in the presence of DTAC. Results at pH 3 and pH 11 without addition of salt.

Experiments at pH 3 and pH 11 were performed in order to understand how the SFG spectrum of water changes with surfactant concentration under either acidic or basic conditions. In

contrast to the results presented in the previous chapter, these experiments were performed without the addition of excess salt. Results at pH 3 without addition of NaCl are presented on Figure 3.4a. According to these results, the SFG spectra increase in intensity in the CH stretching as well as in the OH stretching regions when increasing the DTAC concentration, at concentrations ranging between 2 mM and 20 mM. After this range of DTAC concentrations, the SFG intensity keeps constant until 50 mM of DTAC. As discussed earlier in this chapter, there is substantial overlapping of the CH and the OH resonances, hence SFG experiments in a deuterated solvent were conducted (Section 3.2).

Summarizing the SFG results at pH 3 without addition of salt, in the OH stretching region (3000-3600 cm^{-1}) the increasing SFG intensity is due to the presence of an increasingly positive electrostatic field at the silica/water interface, but at DTAC concentrations higher than 20 mM there is either a saturation of adsorbed DTAC at the interface or if surfactant continues to adsorb above 20 mM DTAC then the resulting change in charge density is compensated for by co-adsorbed chloride. Comparing these results with the results at pH 3 in the presence of 100 mM NaCl (Figure 2.5), a similar trend was observed under higher ionic strength, but the saturation of the silica surface is achieved at a lower concentration (10 mM DTAC). This behavior can be explained by the presence of chloride that decreases the electrostatic repulsion between the positively charged surfactant head-groups, which then permits stronger hydrophobic interactions between the alkyl chains of the surfactant and makes adsorption more thermodynamically favorable. Despite the fact that chloride anion is already in solution because it is the counterion of the surfactant salt, it seems that additional salt further screens the electrostatic repulsion between surfactants in the adlayer.

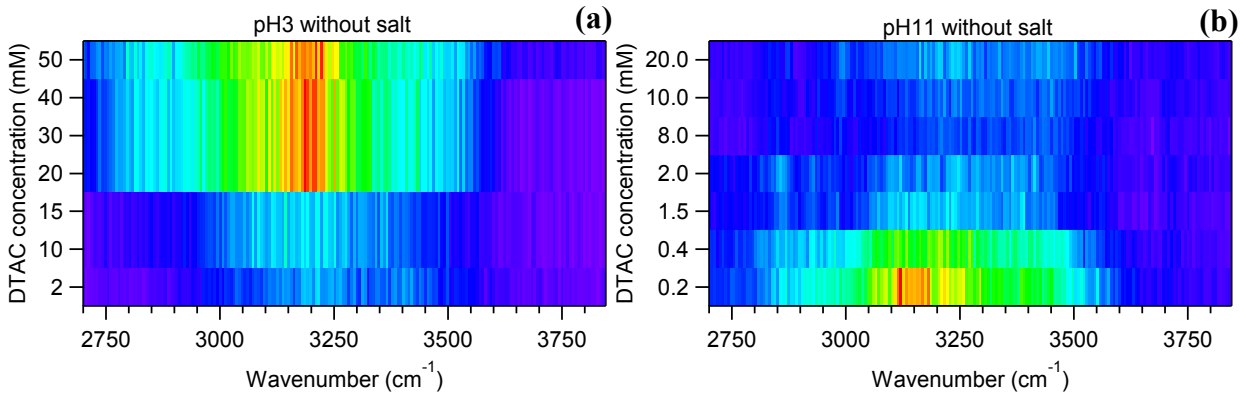

Figure 3.4 SFG spectra in the CH and OH stretching regions for DTAC at pH 3 **(a)** and pH 11 **(b).** The solutions tested were prepared without adding NaCl. The spectra presented in this figure were collected at the silica/H_2O interface. In addition, the spectra are presented as image plots and are not scaled linearly with respect to the DTAC concentration axis.

Panel 3.4b presents the SFG spectra collected at pH 11 for concentrations of surfactant between 0.2 and 20 mM. The SFG intensity in the OH stretching region decreased until a DTAC concentration of 1.5 mM. At higher concentrations of surfactant, the SFG intensity remained relatively low with no significant changes. These results follow the trend described at pH 7 and pH 11 in the presence of NaCl (Figures 2.5b and d**,** respectively), where the adsorption of surfactant reduces the net static electric charge at the interface, and there is no overcompensation of the negative surface charge. In other words, at pH 11 without added salt and at high surfactant concentrations, the positive charge due to the adsorbed surfactant is neutralized by the negative silica surface charge.

.

Conclusion and perspectives

The pH influences not only the characteristics of compounds in the bulk solution but also at interfaces, and it can direct the interactions of these species with the surfaces of minerals. Adsorption of the cationic surfactant DTAC at silica/water interfaces, which have an increasingly negative charge density at pH values above the PZC, is directed by electrostatic interactions between the positively charged quaternary ammonium group of the surfactant and the silanol groups of the silica. At pH values near the PZC, the hydrophobic forces between the adjacent alkyl chains are responsible for surface adsorption and aggregation. At low surfactant concentration, the contact angle and interfacial tension measurements are relatively high. The decrease in contact angle at higher surfactant concentrations, at pH 3, 7 and 11, to a value of 15°, suggests bilayer formation in which the distal leaflet orients the quaternary ammonium group toward the bulk solution rendering the silica/solution interface hydrophilic.

Conformational changes in the DTAC adlayer at the silica/water interface were probed using the interface specific technique, SFG. SFG spectra collected in the CH region (2700-3000 cm^{-1}) were performed using D_2O to avoid overlapping with the OH stretches (3000-3600 cm^{-1}). The methylene and methyl stretches were observed to increase in intensity when increasing the acidity or the alkalinity of the solution containing the DTAC surfactant and 100 mM NaCl. To explain these observations, it is proposed that the surfactant adopts an increasingly noncentrosymmetric structure at the silica/water interface under acidic or basic conditions. Specifically, an unequal distribution of surfactant in the distal and proximal leaflets of the bilayer structure may explain the increase in SFG intensity at pH 3 and 11. Given the results

obtained when fitting the symmetric stretches of the methylene and methyl groups of the surfactant tail with a series of Lorentzian functions, there is not a significant change in the packing of the surfactant tails at basic pH values. However, there is a change in the packing of the surfactant under acidic conditions. In particular, the ratio of the methyl-to-methylene amplitude increases, indicating a change in packing, but further experiments are required to elucidate the nature of this change.

For the SFG spectra in the OH region collected at different surfactant concentrations (including the CMC) with 100 mM NaCl, at pH 3 there was an increase in the SFG intensity suggesting an increase in the electrostatic field at the silica/water interface. A plane of positive charge is created by adsorbed surfactant in the proximal leaflet. This plane will reduce adsorption in the distal leaflet due to electrostatic repulsion, consistent with the SFG results in the CH region as a function of decreasing pH. At pH 11, because of the high negative charge density of the silica surface, the adsorption of the cationic surfactant is more favorable in the proximal leaflet than in the distal leaflet, which explains the increasing SFG intensity in the CH region as the pH increases. Given the results obtained with the contact angle and the interfacial tension measurements that indicated bilayer formation at DTAC concentrations above the CMC, it appears that within the bilayer structure there are different relative amounts of surfactant in each leaflet when the pH is not neutral.

The results presented in this document might be compared with a linear spectroscopic technique such as Raman, in order to quantify the amount of surfactant adsorbed at the solid/water interface and compare those results with the change in the conformation and

aggregation of the adsorbed layers observed in the SFG experiments. Even though for industrial applications the surfactant is not highly purified, SFG experiments studying recrystallized DTAC are recommended to investigate the influence of possible contaminants, such as aliphatic amines, on surfactant aggregates at the silica/water interface. At the same time, the absence of a minimum in the interfacial tension measurements confirms the reasonably high purity of the commercially-bought surfactant used in this study, which was not recrystallized

Given to the interface specificity provided by SFG, studies involving surfactants as well as compounds such as polycyclic aromatic hydrocarbons and organic alkyl acids, which are important components of oil, at silica or alumina based surfaces, could provide additional information about the interactions occurring at mineral interfaces inside oil reservoirs. Understanding these interactions is fundamentally important and will permit the optimization of the concentrations of additives used in hydraulic fracturing fluids, and thus reducing the use and the unnecessary waste of compounds that are potentially harmful for the environment.

References

1. Israelachvili JN. Intermolecular and Surface Forces. 3rd ed. ed: Elsevier Inc; **2011**.

2. Yale School of Engineering & Applied Science http://seas.yale.edu/faculty-research/research-areas/soft-matter-and-complex-fluids **2015**.

3. Rosen MJ. Surfactants and Interfacial phenomena. Hoboken, N J: John Wiley & Sons; **2004**.

4. Maeda H. A thermodynamic analysis of the hydrogen ion titration of micelles. J. Colloid Interface Sci.**2003**,263,277-287.

5. J. Colloid Interface Sci.Molecular-thermodynamic theory of micellization of pH-sensitive surfactants. Langmuir.**2006**,22,3547-3559.

6. Goloub TP, Koopal LK, Bijsterbosch BH, Sidorova MP. Adsorption of Cationic Surfactants on Silica. Surface Charge Effects. Langmuir.**1996**,12,3188-3194.

7. Biswas SC, Chattoraj DK. Kinetics of Adsorption of Cationic Surfactants at Silica-Water Interface. J. Colloid Interface Sci.**1998**,205,12-20.

8. Scott MJ, Jones MN. The biodegradation of surfactants in the environment. Biochim Biophys Acta.**2000**,1508,235-251.

9. Lechuga M, Fernández-Serrano M, Jurado E, Núñez-Olea J, Ríos F. Acute toxicity of anionic and non-ionic surfactants to aquatic organisms. Ecotoxicol. Environ. Saf.**2016**,125,1-8.

10. Olkowska E, Polkowska Z, Ruman M, Namiesnik J. Similar concentration of surfactants in rural and urban areas. Environ Chem Lett.**2015**,13,97-104.

11. Jungermann E. Cationic Surfactants New York **1970**.

12. Dekany I, Szekeres M, Marosi T, Balazs J, Tombacz E. Interaction between ionic surfactants and soil colloids - adsorption, wetting and structural properties. In: Schwuger MJ, Haegel FH, editors. Surfactants and Colloids in the Environment. Progress in Colloid and Polymer Science. 95. Berlin 33: Dr Dietrich Steinkopff Verlag,**1994**,p.73-90.

13. Lyklema J. Adsorption of ionic surfactants on clay minerals and new insights in hydrophobic interactions. In: Schwuger MJ, Haegel FH, editors. Surfactants and Colloids in the Environment. Progress in Colloid and Polymer Science. 95. Berlin 33: Dr Dietrich Steinkopff Verlag,**1994,** p. 91-97.

14. Haigh SD. A review of the interaction of surfactants with organic contaminants in soil. Sci Total Environ.**1996**,185,161-170.

15. Salehi M, Johnson SJ, Liang JT. Mechanistic Study of Wettability Alteration Using Surfactants with Applications in Naturally Fractured Reservoirs. Langmuir.**2008**,24,14099-14107.

16. Austad T, Matre B, Milter J, Sevareid A, Oyno L. Chemical flooding of oil reservoirs 8. Spontaneous oil expulsion from oil- and water-wet low permeable chalk material by imbibition of aqueous surfactant solutions. Colloids Surf A: Physicochem Eng Aspects. **1998**,137,117-129.

17. Woods BL, Walker RA. pH Effects on Molecular Adsorption and Solvation of p-Nitrophenol at Silica/Aqueous Interfaces. J. Phys. Chem. A.**2013,**117,6224-6233.

18. Atkin R, Craig VSJ, Wanless EJ, Biggs S. Mechanism of cationic surfactant adsorption at the solid-aqueous interface. Adv Colloid Interfac.**2003**,103,219-304.

19. Wang YF, Xu HM, Yu WZ, Bai BJ, Song XW, Zhang JC. Surfactant induced reservoir wettability alteration: Recent theoretical and experimental advances in Enhanced Oil Recovery. Pet Sci.**2011**,8,463-476.

20. Ong SW, Zhao XL, Eisenthal KB. Polarization of water molecules at a charged interface second harmonic studies of the silica/water interface. Chem Phys Lett. **1992**,191,327-335.

21. Darlington AM, Gibbs-Davis JM. Bimodal or Trimodal? The Influence of Starting pH on Site Identity and Distribution at the Low Salt Aqueous/Silica Interface. J. Phys. Chem.C. **2015**,119,16560-16567.

22. Ong SW, Zhao XL, Eisenthal KB. Polarization of water-molecules at a charged interface - 2nd harmonic studies of the silica water interface. Chem Phys Lett.**1992**,191,327-335.

23. Allen LH, Matijevíc E, Meites L. Exchange of Na^+ for the silanolic protons of silica. J. Inorg. Nucl. Chem.**1971**,33,1293-1299.

24. Kosmulski M. The pH-Dependent Surface Charging and the Points of Zero Charge. J Colloid Interf Sci. **2002**,253,77-87.

25. Zhang R, Somasundaran P. Advances in adsorption of surfactants and their mixtures at solid/solution interfaces. Adv Colloid Interface Sci. **2006**,123,213-229.

26. Hou BF, Wang YF, Huang Y. Mechanism and Influencing Factors of Wettability Alteration of Water-Wet Sandstone Surface by CTAB. J Dispersion Sci Technol. **2015**,36,1587-1594.

27. Velegol SB, Fleming BD, Biggs S, Wanless EJ, Tilton RD. Counterion effects on hexadecyltrimethylammonium surfactant adsorption and self-assembly on silica. Langmuir. **2000**,16,2548-2556.

28. Liljeblad J. Quaternary Ammonium Surfactants Adsorbed at the Solid-Liquid Interface: A VSFS-Study Master of Science Thesis at the Royal Institute of Technology **2007**.

29. Gragson de, McCarty BM, Richmond GL. Ordering of interfacial water molecules at the charged air/water interface observed by vibrational sum frequency generation. J Am Chem Soc. **1997**,119,6144-6152.

30. Lambert AG, Davies PB, Neivandt DJ. Implementing the theory of sum frequency generation vibrational spectroscopy: A tutorial review. Appl Spectrosc Rev. **2005**,40,103-145.

31. Tyrode E, Rutland MW, Bain CD. Adsorption of CTAB on Hydrophilic Silica Studied by Linear and Nonlinear Optical Spectroscopy. J Am Chem Soc. **2008**,130,17434-17445.

32. Guyot-Sionnest P, Hunt JH, Shen YR. Sum-frequency vibrational spectroscopy of a langmuir film: study of molecular orientation of a two-dimensional system. Phys Rev Lett. **1987**,59,1597-1600.

33. Conboy JC, Messmer MC, Richmond GL. Effect of alkyl chain length on the conformation and order of simple ionic surfactants adsorbed at the D_2O/CCl_4 interface as studied by sum-frequency vibrational spectroscopy. Langmuir.**1998**,14,6722-6727.

34. Bell GR, Bain CD, Ward RN. Sum-frequency vibrational spectroscopy of soluble surfactants at the air/water interface. J Chem Soc-Faraday Trans.**1996**,92,515-523.

35. Bain CD. Sum-frequency vibrational spectroscopy of the solid-liquid interface. J Chem Soc-Faraday Trans. **1995**,91,1281-1296.

36. McBain AJ, Ledder RG, Moore LE, Catrenich CE, Gilbert P. Effects of quaternary-ammonium-based formulations on bacterial community dynamics and antimicrobial susceptibility. Appl Environ Microbiol.**2004**,70,3449-3456.

37. Kandadai MA, Mohan P, Lin G, Butterfield A, Skliar M, Magda JJ. Comparison of Surfactants Used to Prepare Aqueous Perfluoropentane Emulsions for Pharmaceutical Applications. Langmuir.**2010**,26,4655-4660.

38. Chase B, Chmilowski W, Marcinew R, Mitchell C, Dang Y, Krauss K, et al. Clear Fracturing Fluids for Increaed Well Productivity. Oilfield Rev.**1997**,9,20.

39. Liphard M, Vonrybinski W, Schreck B. The role of surfactants and polymers in the filler flotation from waste paper. In: Schwuger MJ, Haegel FH, editors. Surfactants and Colloids in the Environment. Progress in Colloid and Polymer Science. 95. Berlin 33: Dr Dietrich Steinkopff Verlag.**1994**. p. 168-174.

40. Liu JF, Ducker WA. Surface-induced phase behavior of alkyltrimethylammonium bromide surfactants adsorbed to mica, silica, and graphite. J Phys Chem B.**1999**,103,8558-8567.

41. Pons-Jiménez M, Cisneros-Dévora R, Gómez-Balderas R, Cartas-Rosado R, Oviedo-Roa R, Beltrán HI, et al. Supramolecular pairing among heteroaromatic compounds and the cationic surfactant C_{12}TAC. Fuel.**2015**,149,174-183.

42. ShamsiJazeyi H, Verduzco R, Hirasaki GJ. Reducing adsorption of anionic surfactant for enhanced oil recovery: Part I. Competitive adsorption mechanism. Colloid Surf. A. **2014**,453,162-167.

43. Arnaud CH., Figuring out fracking wastewater.Chem Eng News.**2015**,93,8-12.

44. Brown GE. Surface science - How minerals react with water. Science.**2001**,294,67-70.

45. Azam MS, Weeraman CN, Gibbs-Davis JM. Specific Cation Effects on the Bimodal Acid–Base Behavior of the Silica/Water Interface. J Phys Chem Lett.**2012**,3,1269-1274.

46. Covert PA, Jena KC, Hore DK. Throwing Salt into the Mix: Altering Interfacial Water Structure by Electrolyte Addition. J Phys Chem Lett.**2014,**5,143-148.

47. Jena KC, Covert PA, Hore DK. The Effect of Salt on the Water Structure at a Charged Solid Surface: Differentiating Second- and Third-order Nonlinear Contributions. J Phys Chem Lett.**2011,**2,1056-1061.

48. Dewan S, Yeganeh MS, Borguet E. Experimental Correlation Between Interfacial Water Structure and Mineral Reactivity. J Phys Chem Lett.**2013**,4,1977-1982.

49. Dewan S, Carnevale V, Bankura A, Eftekhari-Bafrooei A, Fiorin G, Klein ML, et al. Structure of Water at Charged Interfaces: A Molecular Dynamics Study. Langmuir. **2014**,30,8056-8065.

50. Koopal LK, Goloub T, de Keizer A, Sidorova MP. The effect of cationic surfactants on wetting, colloid stability and flotation of silica. Colloid Surf. A.**1999**,151,15-25.

51. Gomez-Grana S, Hubert F, Testard F, Guerrero-Martinez A, Grillo I, Liz-Marzan LM, et al. Surfactant (Bi)Layers on Gold Nanorods. Langmuir.**2012**,28,1453-1459.

52. Ge J, Feng A, Zhang G, Jiang P, Pei H, Li R, et al. Study of the Factors Influencing Alkaline Flooding in Heavy-Oil Reservoirs. Energy Fuels.**2012**,26,2875-2882.

53. Hayes PL, Keeley AR, Geiger FM. Structure of the Cetyltrimethylammonium Surfactant at Fused Silica/Aqueous Interfaces Studied by Vibrational Sum Frequency Generation. J Phys Chem B.**2010,**114,4495-4502.

54. Abdallah WB, J. S.; Carnegie, A.; Edwards, J.; Herold, B.; Fordham, E.; Graue, A.; Habashy, T.; Seleznev, N.; Signer, C.; Hussain, H.; Montaron, B.; Ziauddin, M. . Fundamentals of Wettability. Oilfied Rev.**2007**,19,44– 61.

55. Duval Y, Mielczarski JA, Pokrovsky OS, Mielczarski E, Ehrhardt JJ. Evidence of the Existence of Three Types of Species at the Quartz−Aqueous Solution Interface at pH 0−10: XPS Surface Group Quantification and Surface Complexation Modeling. J Phys Chem B. **2002**,106,2937-2945.

56. Hayes PL, Chen EH, Achtyl JL, Geiger FM. An Optical Voltmeter for Studying Cetyltrimethylammonium Interacting with Fused Silica/Aqueous Interfaces at High Ionic Strength. J Phys Chem A.**2009**,113,4269-4280.

57. Richmond GL. Molecular Bonding and Interactions at Aqueous Surfaces as Probed by Vibrational Sum Frequency Spectroscopy. Chem Rev. **2002**,102,2693-2724.

58. Somorjai GA. Introduction to Surface Chemistry and Catalysis. New York: John Wiley & Sons; **1994**.

59. Hayes PL, Gibbs-Davis JM, Musorrafiti MJ, Mifflin AL, Scheidt KA, Geiger FM. Environmental Biogeochemistry Studied by Second-Harmonic Generation: A Look at the Agricultural Antibiotic Oxytetracycline. J Phys Chem C. **2007**,111,8796-8804.

60. Fuerstenau DW, Wakamatsu T. Effect of pH on the adsorption of sodium dodecane-sulphonate at the alumina/water interface. Faraday Discuss Chem Soc. **1975**,59,157-168.

61. Atkin R, Craig VSJ, Biggs S. Adsorption Kinetics and Structural Arrangements of Cetylpyridinium Bromide at the Silica−Aqueous Interface. Langmuir. **2001**,17,6155-6163.

62. Rehfeld SJ. Adsorption of sodium dodecyl sulfate at various hydrocarbon-water interfaces. J Phys Chem. **1967**,71,738-745.

63. Sung W, Kim D, Shen YR. Sum-frequency vibrational spectroscopic studies of Langmuir monolayers. Curr Appl Phys. **2013**,13,619-632.

64. Esenturk O, Walker RA. Surface vibrational structure at alkane liquid/vapor interfaces. J Chem Phys. **2006**,125,174701(1-12).

65. Yeganeh MS, Dougal SM, Pink HS. Vibrational Spectroscopy of Water at Liquid/Solid Interfaces: Crossing the Isoelectric Point of a Solid Surface. Phys Rev Lett. **1999**,83,1179-1182.

66. Brown GE, Henrich VE, Casey WH, Clark DL, Eggleston C, Felmy A, et al. Metal Oxide Surfaces and Their Interactions with Aqueous Solutions and Microbial Organisms. Chem Rev. **1999**,99,77-174.

67. Tarbuck TL, Ota ST, Richmond GL. Spectroscopic Studies of Solvated Hydrogen and Hydroxide Ions at Aqueous Surfaces. J Am Chem Soc. **2006**,128,14519-14527.

68. Tian C, Ji N, Waychunas GA, Shen YR. Interfacial Structures of Acidic and Basic Aqueous Solutions. J Am Chem Soc. **2008**,130,13033-13039.

69. Imamura T, Ishiyama T, Morita A. Molecular Dynamics Analysis of NaOH Aqueous Solution Surface and the Sum Frequency Generation Spectra: Is Surface OH– Detected by SFG Spectroscopy? J Phys Chem C. **2014**,118,29017-29027.

70. Ishiyama T, Imamura T, Morita A. Theoretical Studies of Structures and Vibrational Sum Frequency Generation Spectra at Aqueous Interfaces. Chem Rev **2014**,114,8447-8470.

71. Imae TI, S. Characteristics of Rodlike Micelles of Cetyltrimethylammonium Chloride in Aqueous NaCl Solutions - Their Flexibility and the Scaling Laws in Dilute and Semidilute Regimes Colloid Polym Sci. **1987**,265,1090– 1098.

72. Fragneto G, Thomas RK, Rennie AR, Penfold J. Neutron Reflection from Hexadecyltrimethylammonium Bromide Adsorbed on Smooth and Rough Silicon Surfaces. Langmuir. **1996**,12,6036-6043.

73. Speranza F, Pilkington GA, Dane TG, Cresswell PT, Li P, Jacobs RMJ, et al. Quiescent bilayers at the mica-water interface. Soft Matter. **2013**,9,7028-7041.

74. Brown KL, Conboy JC. Electrostatic Induction of Lipid Asymmetry. J Am Chem Soc. **2011**,133,8794-8797.

75. Wang J, Chen C, Buck SM, Chen Z. Molecular Chemical Structure on Poly(methyl methacrylate) (PMMA) Surface Studied by Sum Frequency Generation (SFG) Vibrational Spectroscopy. J Phys Chem B. **2001**,105,12118-12125.

76. Covington AK, Paabo M, Robinson RA, Bates RG. Use of the glass electrode in deuterium oxide and the relation between the standardized pD (paD) scale and the operational pH in heavy water. Analytical Chemistry. **1968**,40,700-706.

77. Torres LL, Chauveau M, Hayes PL. Macromolecular Structure of Dodecyltrimethylammonium Chloride at the Silica/Water Interface Studied by Sum Frequency Generation Spectroscopy. J Phys Chem C. **2015**,119,23917-23927.